1996

A Coupled, Non-Linear, Steady State Model for Early Diagenetic Processes in Pelagic Sediments

Surya P. Dhakar
Old Dominion University

David J. Burdige
Old Dominion University, dburdige@odu.edu

Original Publication Citation

Dhakar, S.P., & Burdige, D.J. (1996). Coupled, non-linear, steady state model for early diagenetic processes in pelagic sediments. *American Journal of Science, 296*(3), 296-330. doi: 10.2475/ajs.296.3.296

[AMERICAN JOURNAL OF SCIENCE, VOL. 296, MARCH, 1996, P. 296–330]

A COUPLED, NON-LINEAR, STEADY STATE MODEL FOR EARLY DIAGENETIC PROCESSES IN PELAGIC SEDIMENTS

SURYA P. DHAKAR and DAVID J. BURDIGE
Department of Oceanography, Old Dominion University, Norfolk, Virginia 23529

ABSTRACT. A steady state, coupled, non-linear model has been developed for early diagenetic processes in pelagic and hemi-pelagic marine sediments. Model results show that the occurrence of oxic and sub-oxic diagenetic processes is significantly affected by variations in parameters such as the sedimentation rate, bioturbation coefficient, sediment porosity, and organic matter flux to the sediments. Increases in the sedimentation rate or the bioturbation coefficient increase organic matter oxidation by sub-oxic processes, whereas an increase in sediment porosity decreases organic matter oxidation by sub-oxic processes. Sediment data from three contrasting MANOP sites are fit reasonably well with the model. The resulting best-fit organic carbon, oxygen, and nitrate fluxes at the sediment-water interface and depth-integrated organic carbon oxidation rates for these sites are also within the range of independent estimates of these quantities.

Model results show that the internal redox cycling of manganese in sediments leads either to the formation of a Mn-peak near the sediment redox boundary or to surficial Mn-rich oxic sediments, depending on the depth zonation of manganese oxidation and bioturbation. In sediments with a shallow redox boundary (<5 cm), upward diffusion of pore water manganese into the oxic sediments dominates over manganese oxidation near the redox boundary. The majority of the manganese oxidation therefore occurs in the surficial, bioturbated sediments, and as a result, manganese-rich oxic sediments are formed. In contrast, in sediments with a deeper redox boundary (>10 cm), manganese oxidation near the sediment redox boundary dominates over pore water manganese diffusion into the overlying oxic sediments. Here, the majority of the manganese oxidation occurs below the zone of active bioturbation (assumed to be the upper 8-10 cm of sediment), and in this case, a well developed Mn-peak forms near the sediment redox boundary. Previous models explained the occurrence of this Mn-peak by neglecting bioturbation or suggested that this peak could not occur in bioturbated sediments due to this sediment mixing.

I. INTRODUCTION

The remineralization (oxidation) of organic matter in recent marine sediments has a significant influence on the global cycling of many elements such as carbon, nitrogen, phosphorus, manganese, iron, and other related metals (Froelich and others, 1979; Emerson and others, 1985; Burdige, 1993). This remineralization is coupled to the reduction of various electron acceptors (oxygen, nitrate, manganese and iron oxides, and sulfate), the occurrence of which are apparently controlled, at a first order level, by the free energy yield per mole of organic carbon oxidized for each of these processes (Froelich and others, 1979; Strumm

and Morgan, 1981). Studies in recent years have begun to elucidate further the factors that control not only the occurrence of these processes but also appear to affect the ultimate preservation (or permanent burial) of organic matter in pelagic sediments. These include sedimentation and bioturbation rates, the bottom water oxygen concentration, and the organic matter flux to the sediment surface (Froelich and others, 1979; Bender and Heggie, 1984; Emerson and others, 1985; Emerson and Hedges, 1988; Canfield, 1993).

One approach to the study of remineralization processes in sediments has involved the use of mathematical models, and models of varying degree of complexity have been presented (Berner, 1980; Goloway and Bender, 1982; Jahnke and others, 1982a; Burdige and Gieskes, 1983; Emerson and others, 1985; Gratton and others, 1990; Rabouille and Gaillard, 1991a, 1991b; and others). While these models have had certain successes in quantifying aspects of organic matter remineralization in sediments, they also have certain limitations. For example, in some models developed to examine sediments in which there is an upper oxic zone (where aerobic respiration occurs) and a deeper sub-oxic zone (where denitrification, Mn and/or Fe reduction may occur) separate sets of equations are used for each of these regions. This requires that the depth of oxygen penetration (or redox boundary), which separates the oxic and sub-oxic zone, be externally specified (Goloway and Bender, 1982; Jahnke and others, 1982b; Burdige and Gieskes, 1983). In addition, simplifying assumptions have often been made for various physical and biochemical processes occurring in the sediments (for example, sediment mixing or bioturbation is assumed to be constant over a fixed depth in the sediments; the kinetics of organic matter oxidation is assumed to be independent of electron acceptor concentration and only dependent on the amount of metabolizable organic carbon present).

Some of these problems are illustrated by examining the ways that these diagenetic models handle the effects of bioturbation on the distribution of Mn in pelagic sediments. While it is well known that a solid phase Mn-peak occurs in many Equatorial Atlantic and Pacific sediments just above the sediment redox boundary (Froelich and others, 1979; Berger and others, 1983; Murray, 1987; Finney, Lyle, and Heath, 1988; Price, 1988; Burdige, 1993), previous models could only explain the formation of these peaks by neglecting bioturbation (Burdige and Gieskes, 1983). In contrast, models that incorporate bioturbation tend to disperse this Mn-peak (Gratton and others 1990; Rabouille and Gaillard, 1991b). Rabouille and Gaillard (1991b) suggested that this apparent contradiction between the occurrence of bioturbation and well developed Mn-peaks in some sediments may be caused by non-steady state diagenetic processes. However, it is also likely that this may result from the ways in which bioturbation is quantified in these models.

Rabouille and Gaillard (1991b) presented a steady state diagenetic model that includes oxidation of organic matter by a continuous sequence of electron acceptors (oxygen, nitrate, and Mn oxides) and also

used modified forms of the Monod law to describe the kinetics of organic matter oxidation by each of these processes (see sect. III.C.2 for further details). This latter approach more appropriately incorporates the dependence of electron acceptor concentrations on the rates of these processes (see the discussion below). In their model they also multiplied the rate expressions for the sub-oxic processes, denitrification, and Mn reduction, by an inhibition factor that is a function of oxygen concentration. This allowed them to use a single equation for each chemical constituent over the entire sediment column (that is, in both oxic and sub-oxic zones) and led to the observed biogeochemical zonation of these processes in the sediments without externally specifying the sediment redox boundary. However, in spite of the advances made with this approach, this model still had certain difficulties in explaining the formation of a Mn-peak near the sediment redox boundary (see the discussion above).

In this paper we present a steady-state diagenetic model for organic matter remineralization in pelagic sediments which overcomes many of these problems. This model includes organic matter oxidation by electron acceptors in both the oxic and sub-oxic zones, as well as other chemical and biological reactions known to occur in these sediments (for example, nitrification, Mn oxidation, and Mn reduction coupled to Fe^{2+} oxidation). In addition, a new mathematical approach is used in this model to describe the depth dependence of bioturbation in sediments. With this new approach the formation of a Mn-rich layer near the sediment redox boundary of bioturbated sediments can now be explained. This model will also be applied to data from several Pacific pelagic sediments, and the results of these calculations will be compared to other studies of carbon cycling and remineralization in these sediments.

II. THE MODEL—GENERAL CONSIDERATIONS

The generalized diagenetic equation on which this model is based can be written as follows (Berner, 1980; Rabouille and Gaillard, 1991b):

$$\frac{\partial C}{\partial t} = \frac{\partial}{\partial x}\left[(D + K_b)\frac{\partial C}{\partial x} - \omega C\right] \pm \sum R \qquad (1)$$

where:

C = the bulk sediment concentration of a species in either the solid or dissolved phase
x = depth (positive downward)
t = time
ω = sedimentation rate
D = the bulk sediment diffusion coefficient (for solids this is assumed to be equal to zero)
K_b = the bioturbation coefficient
R = production/consumption of species C in biogeochemical reactions

Transport processes in this model include molecular diffusion (dissolved species only), advection, and sediment mixing by bioturbation. This approach also assumes that sediments are laterally homogeneous and only vary vertically. Additional details of the general assumptions of this modeling approach are discussed in Berner (1980).

Rate expressions in the model are developed in a way similar to that described in Rabouille and Gaillard (1991b), such that the occurrence or non-occurrence of a given process is directly determined by chemical distributions in the sediments. This then eliminates the need to write separate differential equations for each chemical constituent in different sediment zones (see sect. III.C.3 for further details).

III. PHYSICAL AND BIOCHEMICAL PROCESSES IN THE MODEL

A. Physical Processes

1. Molecular diffusion.—Molecular diffusion is the dominant process by which dissolved materials are transported in the pore waters of marine sediments (Berner, 1980). The bulk sediment diffusion coefficient (D_s) can be expressed as $D_o/\phi F$, where D_o is the free ion molecular diffusion coefficient, ϕ is the sediment porosity, and F is the formation factor that measures the tortuosity of the sediment matrix with regard to molecular diffusion (McDuff and Ellis, 1979; Berner, 1980). According to Ullman and Aller (1982) $F \approx \phi^{-3}$ for high porosity ($\phi \geq 0.7$) unconsolidated, marine sediments. Therefore, in this model we have assumed,

$$D_s = D_o * \phi^2 \tag{2}$$

2. Advection.—The advection of solids and pore waters in the sediments occurs as a result of deposition of new material at the sediment-water interface (sedimentation) and is further affected after deposition by compaction of the sediments with depth. Compaction leads to a decrease with depth in sediment porosity, along with a decrease in the advection rate of solids and an increase in the advection rate of pore waters (Berner, 1980). However, the extent to which compaction affects biogeochemical processes in sediments (and therefore should be included in diagenetic models of these processes) is subject to some uncertainty. Rabouille and Gaillard (1991a) observed that the inclusion of compaction in their diagenetic model led to significant differences in the depth of oxygen penetration and carbon preservation in the sediments. However, in this and later studies (Rabouille and Gaillard, 1991b), they assumed that changes in compaction affected only advection of solids and neglected to incorporate similar changes in bulk sediment diffusion coefficients brought about by decreases in porosity (based on eq 2, a decrease in ϕ with depth leads to a decrease in D_s). This discrepancy suggests that it is difficult to

ascertain the importance of compaction on biogeochemical processes in pelagic sediments based on the results of their calculations. In our model then, we therefore have assumed that porosity is constant with depth and that the advection rate of both pore waters and solids in these sediments is the same as the sedimentation rate.

B. Bioturbation

Bioturbation is defined as the displacement of sediment grains as a result of the activity of benthic and infaunal organisms (Richter, 1952). In this model, as in earlier studies, bioturbation is assumed to be a random, diffusion-like process, in which mixing occurs via a large number of small, random steps (see Boudreau, 1986a and references cited therein). This assumption appears to describe particle mixing reasonably well in deep sea sediments (Boudreau, 1986a; Aller, 1990; Wheatcroft and others, 1990; Smith, 1992). In pelagic sediments, where sedimentation rates are low ($\approx$ 1cm/kyr), bioturbation is often a more important transport process than sedimentation in the upper portions of the sediments (Guinasso and Schink, 1975; Emerson and others, 1985; Boudreau, 1986b). Bioturbation can therefore transfer reactive organic carbon to the deeper parts of sediment and thus significantly influence not only the occurrence of oxic and sub-oxic diagenesis but also the preservation of sedimentary organic matter (Berner, 1980; Emerson and others, 1985; Stordal and others, 1985; Boudreau, 1986a; Aller, 1990; Coppedge and Balsam, 1992; Smith and others, 1993). In our model, conveyor belt-like transport by deposit feeders (Aller, 1982; Robbins, 1986) and bioirrigation (Boudreau, 1984; Aller and Yingst, 1985) have also been neglected, since they do not appear to have a significant effect on oxic and sub-oxic processes in pelagic sediments (Aller, 1990).

Earlier studies indicated that rates of sediment mixing are controlled by macrofaunal abundance, and that mixing rates decrease as the numbers of macrofauna decrease (Rhoads, 1974; Li and others, 1985; Levin, Huggett, and Wishner, 1991). Furthermore, these studies suggested that the presence of oxygen affects the occurrence of macrofauna in sediments (Rhoads, 1974; Levin, Huggett, and Wishner, 1991), and that significant macrofaunal activity occurs only above the sediment redox boundary (Rhoads, 1974; note that here we define the sediment redox boundary as the depth in the sediments where pore water oxygen goes to near zero levels, Burdige, 1993). Laboratory studies of Rhoads (1974) demonstrated that a decrease in the depth of the sediment redox boundary drives benthic macrofauna to the sediment surface, while laboratory studies with the *Eupolymnia* polychaete showed that their burrowing activities increase in the presence of oxygen (Marinelli, 1994). The depth and intensity of sediment mixing, therefore, appears to be strongly influenced by the depth to which macrofauna are significantly present in the sediments; this suggests that the most intense sediment mixing occurs above the sediment redox boundary, with the rates of mixing decreasing

in sub-oxic and anoxic zones. (Rhoads, 1974; Kadko and Heath, 1984; Aller, 1990; Levin, Huggett, and Wishner, 1991).

Several studies have shown that the maximum amounts of bioturbation occur in the upper 8 to 10 cm of pelagic sediments and then decrease rapidly with depth (Berger and Killingley, 1982; Kadko and Heath, 1984; Cochran, 1985; Li and others, 1985; Boudreau, 1986a; Aller, 1990; Rutgers van der Loeff, 1990; Levin, Huggett, and Wishner, 1991; Smith and others, 1993). The statistical analysis in Boudreau (1994) supports this observation, showing that the depth of the mixed layer in pelagic sediments (based on radiochemical measurements) has a "well-defined mean" of 9.8 cm (±4.5 cm). Although benthic macrofaunal burrows in pelagic sediments may be present at deeper depths (Rhoads, 1974; Li and others, 1985; Aller, 1994), Jumars and Wheatcroft (1989) discuss the increasing energy costs to benthic macrofauna of burrowing deeper than 10 to 15 cm. While this might be taken as "defining" the maximum depth of bioturbation or sediment mixing in pelagic sediments, the discussion above suggests that the depth of oxygen penetration should also affect the depth of sediment mixing.

The factors controlling bioturbation and sediment mixing are complex (Levin, Huggett, and Wishner, 1991; Smith and others, 1993; Aller, 1990, 1994; Boudreau, 1994), and with our present knowledge it is difficult to ascertain what other factors, besides oxygen, may control the depth dependence of the bioturbation coefficient at a given site. Previous workers have generally assumed that bioturbation coefficients are highest in the surface sediments and decrease rapidly below some depth (that is, the sediment mixed layer; Li and others, 1985; Murray and Kuivila, 1990; Rabouille and Gaillard, 1991a, b). However this approach can allow equivalent rates of sediment mixing to occur in both oxic and sub-oxic sediments. In our model we have therefore assumed that significant sediment mixing occurs down to the depth of the sediment redox boundary or to a maximum depth of 8 cm, and that sediment mixing then gradually decreases with depth. As we will show, model results with this assumption are consistent with field data from contrasting MANOP sites. Furthermore this formalism also allows us to explain the distribution of solid phase Mn in various sediment cores. At the same time though, we recognize that further laboratory and field studies on the factors controlling the depth-dependence of sediment mixing are needed to verify our assumption of oxygen-dependent bioturbation.

Based on this assumption the depth dependence of the bioturbation coefficient (K_b^x) is expressed as follows:

$$K_b^x = K_b^\infty + Of_x * \frac{(K_b^0 - K_b^\infty)}{1 + e^{(b_c*(x-x_b))}}. \tag{3}$$

where:

K_b^0 = maximum bioturbation coefficient at the sediment surface
K_b^∞ = minimum bioturbation coefficient deeper in the sediments
b_c = bioturbation "attenuation" constant = 1.0
x = depth in the sediment
x_b = depth of maximum bioturbation
Of_x = oxygen dependent bioturbation inhibition factor.

In completely oxic sediments $Of_x = 1$ (see below), and maximum sediment mixing occurs to a depth of 8 cm and then gradually reduces to an insignificant value deeper in the sediments[1] (see fig. 1A). Interestingly, this depth dependence of K_b leads to a sediment mixed layer that is ≈2 to

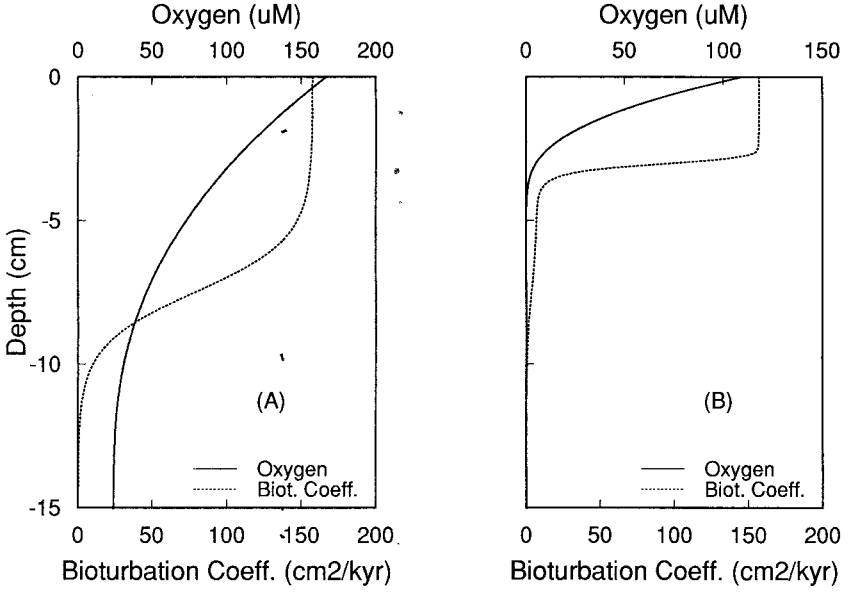

Fig. 1. The effect of oxygen (solid lines) on the depth-dependence of bioturbation (dotted lines) for two hypothetical oxygen profiles. (A) Bioturbation is controlled by sediment depth when oxygen is present below the depth of maximum bioturbation x_b (8 cm). (B) Bioturbation is controlled by oxygen when oxygen is consumed above x_b. As discussed in the text in both cases, this approach leads to a model determined sediment mixed layer (based on either the model derived excess ^{210}Pb penetration depth or depth of constant ^{14}C activity) that is ≈2 to 3 cm deeper than the depth at which K_b begins to decrease (8 cm in fig. 1A and ≈4 cm in fig. 1B).

[1] Although strictly speaking bioturbation should go to zero with depth, the nature of our numerical scheme requires that the bioturbation coefficient be non-zero at all sediment depths. In practice, however, we set the K_b^∞ equal to 10^{-8} K_b^0, so the net effect is that with depth the bioturbation coefficient effectively goes to zero.

3 cm deeper than the 8 cm depth of maximum K_b (results not shown here; these mixed layer depths are the excess ^{210}Pb penetration depth or depth of constant ^{14}C activity determined by using our model equations to predict the depth profiles of these radiochemicals).

To incorporate the inhibitory effect of oxygen on the rate of sediment mixing in sub-oxic sediments, we use the following inhibition factor (Of_x):

$$Of_x = \frac{1.0}{1.0 + e^{(b_k*(Oxc-Ox))}} \tag{4}$$

where:

b_k = bioturbation inhibition constant = 100.0
Ox = oxygen concentration in the sediment
Oxc = critical oxygen concentration for bioturbation.

We have assumed that the critical oxygen concentration for bioturbation is 4.0 μM, based on arguments in sect. VIII. As discussed above, this inhibition function is equal to 1 in oxic sediments ($[O_2] \geq 4.0$ μM; fig. 1A), although in sediments where oxygen goes to zero above x_b, Of_x decreases the bioturbation coefficient in the absence of oxygen (fig. 1B).

C. Bio-Chemical Processes

1. Proposed reactions.—The dominant reactions proposed to occur in these sediments are oxic and sub-oxic remineralization of sedimentary organic matter (aerobic respiration, denitrification, and Mn and Fe reduction). The stoichiometry we have used for these reactions is that suggested by Froelich and others (1979) and is shown in table 1. Besides organic matter oxidation, the following reactions are also included in the model (also see table 1): Fe^{2+}, Mn^{2+}, and NH_4^+ oxidation (nitrification) by oxygen; Fe^{2+} oxidation by Mn oxides (Postma, 1985; Myers and Nealson, 1988; Burdige, Dhakar, and Nealson, 1992) and NH_4^+ oxidation by nitrate (Goloway and Bender, 1982; Bender and others, 1989).

2. Kinetic formulations.—In many diagenetic models, organic matter degradation rates are considered to be proportional to organic matter concentration and independent of electron acceptor concentrations (Jahnke and others, 1982b; Westrich and Berner, 1984; Emerson and others, 1985; Murray and Kuivila, 1990). However, aerobic respiration appears to be independent of oxygen only above 3 μM concentration (Devol, 1978), suggesting that a modified form of the Monod equation is a more appropriate rate expression for aerobic respiration in sediment systems where the oxygen concentration goes to zero (Rabouille and Gaillard, 1991a, 1991b).

$$R = \frac{k\,G\,C}{K_m + C} \tag{5}$$

TABLE 1

Early diagenetic reactions in pelagic sediments

Organic matter undergoing remineralization is abbreviated by OM:

$$OM = (CH_2O)_{106}(NH_3)_{16}(H_3PO_4)_1 \quad (1)$$

Reactions in the oxic layer of the sediments:

$$OM + 138O_2 \rightarrow 106CO_2 + 16HNO_3 + H_3PO_4 + 122H_2O \quad (2)$$

$$2Mn^{2+} + O_2 + 2H_2O \rightarrow 2MnO_2 + 4H^+ \quad (3)$$

$$2Fe^{2+} + O_2 + 2H_2O \rightarrow 2FeOOH + 2H^+ \quad (4)$$

$$NH_4^+ + 2O_2 \rightarrow NO_3^- + H_2O + 2H^+ \quad (5)$$

Reactions in the sub-oxic layer of the sediments:

$$OM + 94.4HNO_3 \rightarrow 106CO_2 + 55.2N_2 + H_3PO_4 + 177.2H_2O \quad (6)$$

$$OM + 236MnO_2 + 472H^+ \rightarrow 236Mn^{2+} + 106CO_2 + 8N_2 + H_3PO_4 + 366H_2O \quad (7)$$

$$OM + 424FeOOH + 848H^+ \rightarrow 424Fe^{2+} + 106CO_2 + 16NH_3 + H_3PO_4 + 742H_2O \quad (8)$$

$$5NH_4^+ + 3HNO_3 \rightarrow 4N_2 + 9H_2O + 5H^+ \quad (9)$$

$$2H_2O + MnO_2 + 2Fe^{2+} \rightarrow Mn^{2+} + 2FeOOH + 2H^+ \quad (10)$$

$$10Fe^{2+} + 2HNO_3 + 24H_2O \rightarrow 10Fe(OH)_3 + N_2 + 20H^+ \quad (11)$$

where:

k = rate constant for the reaction
K_m = half-saturation constant for the process
C = electron acceptor concentration
G = concentration of metabolizable organic matter

Rabouille and Gaillard (1991b) used an oxygen concentration of 3.1 μM as the half saturation constant for organic matter oxidation by aerobic respiration, consistent with the results of water column studies by Devol (1978). To the best of our knowledge, no other information is available for the K_{ox} value in deep sea sediment. We have therefore also used the same value (3.1 μM) for K_{ox}.

Denitrification rates in sediments also show Monod-type kinetics (Messer and Brezonik, 1984; Nakajima, Hayamizy, and Nishimura, 1984a; Muela and others, 1988), with reported half-saturation constants that range from 10 to 40 μM (Nakajima, Hayamizy, and Nishimura, 1984b); therefore, we have also used eq (5) to describe the kinetics of denitrification. The half-saturation constant we have used, 20 μM, is similar to that used by Rabouille and Gaillard (1991b). The rates of Mn and Fe reduction coupled to organic matter oxidation were assumed to be second

order (Rabouille and Gaillard, 1991b), proportional to the concentrations of organic matter and solid phase manganese or iron oxides.

In our model we have also assumed that there are two fractions of organic matter in these sediments, a metabolizable fraction that is reactive on early diagenetic time scales and a non-metabolizable fraction (Berner, 1980). Preservation of organic matter in these sediments then results from either complete oxidation of all metabolizable organic matter or the complete utilization of all oxidants. In the first case the preserved organic matter is thus the operationally-defined, non-metabolizable material, while in the second case organic matter that is preserved is now a mixture of non-metabolizable and metabolizable organic matter. Implicit in this formalism is the assumption that organic matter oxidation coupled to sulfate reduction is not an important process in these sediments, based on evidence to date which suggests that sulfate reduction is not a significant early diagenetic process in most pelagic sediments (Bender and Heggie, 1984; Jahnke and others, 1989).

Laboratory studies of Mn oxidation indicate that the process is autocatalytic and proportional to $[Mn^{2+}]$, pH, $[O_2]$, and the concentrations of solid phase Mn oxide (Morgan, 1967; Yeats and Strain, 1990). However, the results of Taylor (1986) suggest that sedimentary Mn oxidation is proportional to $[Mn^{2+}]$ and independent of O_2 except at low O_2 concentration. The process also appears to be independent of solid phase Mn except at low MnO_2 concentration (Hem, 1981). In our model we therefore have used the following relationship for the kinetics of Mn oxidation:

$$R_m = k_{mox} * [Mn_{pw}] * \frac{[Ox]}{K_{oxm} + [Ox]} \tag{6}$$

where k_{mox} is the rate constant for Mn oxidation, and K_{oxm} is the half-saturation concentration of oxygen for Mn oxidation. Based on sediment slurry experiments, Taylor (1986) estimated a K_{oxm} value of 9.6 μM, although he also suggested that this may be an overestimate of its true value. We have assumed a lower value of K_{oxm} (=1.0 μM) based on observations discussed in sect. VIII.

The kinetics of iron oxidation by oxygen is taken to be first order with respect to both the Fe^{2+} and oxygen concentrations (Millero, Sotolongo and Izaguirre, 1987). We have also assumed that the oxidation of iron by Mn oxides is first order with respect to the Fe^{2+} concentration and the quantity of solid phase Mn oxides present. This is based on laboratory studies that have shown that the rate of the process is dependent on the available surface area of Mn oxides (Postma, 1985; Burdige, Dhakar, and Nealson, 1992). Finally we have assumed that the oxidation of ammonium by oxygen and nitrate is first order with respect to ammonium and either oxygen or nitrate.

3. Inhibition of sub-oxic processes in the presence of oxygen.—The oxidation of organic matter by nitrate (Knowles, 1982; Nakajima, Hayamizy,

and Nishimura, 1984b) and Mn oxides (Ehrlich, 1987) has been shown to be inhibited by the presence of oxygen. Therefore, in the model equations the rate expressions for nitrate and Mn reduction coupled to organic matter oxidation are multiplied by the following inhibition factor, similar to one that is used by Rabouille and Gaillard (1991b),

$$f_x = \frac{1.0}{1.0 + e^{(b_{nm}*(Ox - Oxic))}} \tag{7}$$

where:

b_{nm} = inhibition attenuation constant = 1000.0
Ox = oxygen concentration in the sediment
O_{xic} = the critical oxygen concentration for the inhibition of denitrification and Mn reduction

The results of laboratory and modeling studies suggest that the critical oxygen concentration that inhibits nitrate and Mn reduction varies between 0.1 to 10 μM (Jahnke and others, 1982b; Nakajima, Hayamizy, and Nishimura, 1984b; Rabouille and Gaillard, 1991b). We have therefore assumed here that O_{xic} in eq (7) is equal to 6 μM. We have used the same inhibition factor for both Mn reduction and denitrification, based on studies that suggested these processes can occur simultaneously in many pelagic sediments (Klinkhammer, 1980; Lyle, 1983; Sawlan and Murray, 1983).

Various field studies have shown that iron reduction occurs after oxygen, nitrate, and Mn oxides have been consumed in the sediments (Froelich and others, 1979; Emerson and others, 1980; Klinkhammer, 1980; Bender and Heggie, 1984; Lyle, Heath, and Robbins, 1984; De Lange, 1986; Aller, 1990; Rutgers van der Loeff, 1990). While this observation is consistent with thermodynamic arguments (Froelich and others, 1979; Stumm and Morgan, 1981), the exact mechanism by which iron reduction is inhibited in the presence of electron acceptors such as nitrate and Mn oxides is unclear. It is possible that the presence of these electron acceptors may directly inhibit microbial iron reduction (Sorensen, 1987) in a way similar to that in which the presence of oxygen inhibits sub-oxic remineralization processes. However, in this model we have assumed that microbial Fe reduction can co-occur with denitrification and microbial Mn reduction, and that any Fe^{2+} produced in this fashion is oxidized back to Fe^{3+} by either nitrate or Mn oxides (Myers and Nealson, 1988; Burdige, 1993; see reactions 10 and 11 in table 1). The possible occurrence of these iron oxidation reactions, therefore, leads to the apparent net separation of these sub-oxic processes in spite of their co-occurrence (Burdige, 1993). Furthermore, Fe^{2+} does not accumulate in pore waters in the presence of nitrate and Mn oxides (as is generally seen in field data), and net iron reduction is essentially zero in the zones of Mn reduction and denitrification. Based on this suggestion, we have

consequently assumed that the inhibition factor for iron reduction is the same as that for denitrification and Mn reduction.

IV. DIAGENETIC EQUATIONS AND BOUNDARY CONDITIONS

The specific diagenetic equations for solid phase organic carbon, Mn and Fe, and dissolved (pore water) oxygen, nitrate, Mn, Fe, and ammonia are listed in app. 1. The boundary conditions used to solve the pore water equations assume that pore water concentrations are equal to bottom water values at the sediment-water interface (x = 0), and that the pore water gradients ($\partial C/\partial x$) go to zero as $x \rightarrow \infty$. For solid phase Mn, Fe, and metabolizable organic carbon the upper boundary condition specifies the fluxes of these compounds at the sediment water interface ($F_c = \rho(1 - \phi)(-K_b\, \partial C/\partial x + \omega\, C)_{x=0}$). The lower boundary condition assumes that the gradients of these materials also go to zero as $x \rightarrow \infty$.

V. GENERAL APPROACH TO THE SOLUTION OF THESE EQUATIONS

The coupled, non-linear differential equations in this model have no analytical solutions and can only be solved numerically. We have solved these equations using an implicit numerical iterative procedure, based on a centered finite differencing scheme to approximate the first and second derivatives (Crank, 1975; Roache, 1982; Rabouille and Gaillard, 1991a).[2] The sediment column is divided into n intervals of equal length Δx, and coupled, non-linear rate expressions are linearized and uncoupled using values from the previous iterations (see below). For example, using this approach the differential equation for pore water oxygen (see app. 1) is re-written as,

$$0 = [(D_o\phi^2 + K_{b_i})] \times \left[\frac{Ox_{i-1} - 2Ox_i^{\cdot} + Ox_{i+1}}{\Delta x^2}\right] + \left[\frac{K_{b_{i+1}} - K_{b_{i-1}}}{2\Delta x} - \omega\right] \times \left[\frac{Ox_{i+1} - Ox_{i-1}}{2\Delta x}\right] - R_i\, Ox_i \tag{8}$$

where:

$$R_i = \phi\, \frac{l_{mox} k_{mox} Mn_i^p}{K_{oxm} + Ox_i^p} + \frac{\rho(1 - \phi) k_{ar} G_i^p}{K_{ox} + Ox_i^p} + \phi l_{fox} k_{fox} Fe_i^p + \phi\, l_{ao} k_{ao} A_{m_i}^p, \tag{9}$$

and the superscipt p represents the value of this quantity from the previous iteration. For each chemical constituent this then leads to n equations of the form,

$$0 = b_i C_{i-1} + a_i C_i + c_i C_{i+1} \tag{10}$$

where a_i, b_i and c_i are coefficients determined by re-arranging terms in equations such as eq (8). In addition, the first and last equations of each

[2] Note that a copy of the FORTRAN code used to solve these equations is available by writing to the senior author (DJB).

set of n equations are rewritten based on the boundary conditions (see app. 2). These equations can be expressed in the form of a tri-diagonal matrix and solved by Gaussian elimination (Press and others, 1992). In our approach to solving these equations, an initial "guess" is made for the depth profile of each constituent, and these initial profiles are then used as discussed above to solve for a new set of solutions (that is, concentration versus depth profile for each constituent). The results from previous calculations are iteratively used to recalculate a new set of concentration values until successive solutions differ by less than 0.001 percent.

The validity of the numerical solutions was checked by comparing numerical and analytical solutions of linearized forms of the equations in app. 1. We linearized the organic carbon and oxygen equations by modifying the reaction term such that the organic matter degradation rate was independent of oxygen concentration and simply first order with respect to organic matter concentration. Analytical and numerical solutions to these equations agreed very well, differing by less than 0.1 percent.

Internal consistency of the numerical solutions was also examined in the following mass balance calculations. For total organic carbon this involved comparing the carbon flux to the sediment surface (OMF) with the carbon burial rate (OMB) and the depth-integrated carbon oxidation rate (OCR) by the various electron acceptors. Under steady-state conditions, the following equality should hold:

$$OMF = OMB + OCR \tag{11}$$

For other compounds such as oxygen, Mn, and nitrogen, this mass balance calculation involved comparing the flux across the sediment surface with the sum of the burial rate below the zone of early diagenesis and the net depth-integrated production or consumption rate within the sediments. By analogy with eq (11), the first value should equal the latter sum. For any given model run these mass balance calculations agreed to within less than 0.5 percent.

VI. MODEL RESULTS

In initial model runs we examined how variations in the organic matter flux to the sediment surface, the sediment porosity, the bioturbation coefficient, and the sedimentation rate affect organic matter remineralization in sediments.

At low organic carbon fluxes, the sediments are carbon "limited" and, therefore, completely oxic (fig. 2A and B). Sub-oxic processes do not occur, pore waters show a slight increase in nitrate concentration due to nitrification (fig. 2C), and dissolved Mn and Fe are absent. As the carbon flux to the sediments increases, the sediments become oxygen "limited," and sub-oxic respiration processes occur (fig. 2F-J). This also leads to Mn redox cycling across the sediment redox boundary and results in a Mn-peak in the sediments (fig. 2I). The results in figure 2I and J also show that the oxygen half saturation constant for organic matter oxida-

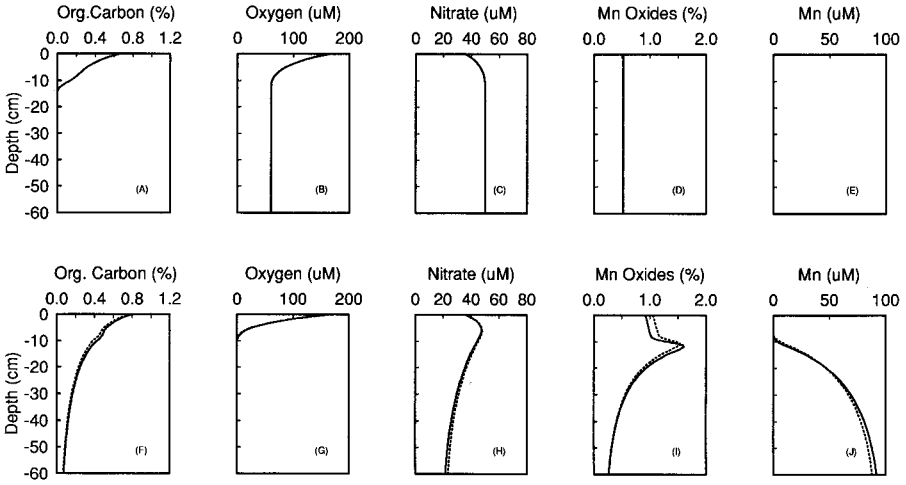

Fig. 2. Model distributions of organic carbon, oxygen, nitrate, and manganese, all versus depth. The top row (a-e) shows results for a low organic carbon flux to the sediments (25 mmol/m^2/yr). These sediments are completely oxic, and no sub-oxic diagenetic processes occur. The bottom row (f-j) shows results for a higher organic carbon flux to the sediments (47 mmol/m^2/yr). Both oxic and sub-oxic diagenetic processes occur in these sediments and lead to the formation of a manganese peak near the sediment redox boundary. Solid and dotted lines are profiles determined by the model with K_{ox} values of 6.0 and 3.1 μM respectively. The other parameters used in these model calculations are listed in table 2 for site S (top row) and site C (bottom row). Note that in these and all other model runs, calculations are performed to a depth of 150 cm to allow all pore water and solid phase concentration gradients to go to zero (that is, to satisfy the lower boundary condition for the model equations discussed in sec V). However to aid in visualizing our results, we only show profiles for the upper 20 to 40 cm, since these profiles show minimum changes below these depths.

tion (K_{ox}) has a slight influence on the formation of this Mn-peak and on the Mn pore water profiles, although it has a relatively insignificant effect on the oxygen and nitrate pore water profiles. An examination of eq (5) indicates that as oxygen concentrations approach zero, the rate of aerobic respiration decreases more rapidly at a K_{ox} value of 6.0 μM versus 3.1 μM. This larger K_{ox} value then leads to a small increase in the oxygen penetration depth, the amount of organic carbon available for sub-oxic oxidation, and the amount of oxygen available for Mn^{2+} and Fe^{2+} oxidation. This increases the amount of Mn redox cycling in the sediments and results in a slightly larger Mn-peak that is somewhat deeper in the sediments.

The results in figure 3 show that variations in sediment porosity have significant effects on the occurrence of oxic and sub-oxic processes in the sediments. At higher porosities, bulk sediment diffusion coefficients increase, leading to higher fluxes of oxygen into the sediments. Therefore with increasing porosity organic matter oxidation by aerobic respiration increases, while organic matter oxidation by sub-oxic respiration

TABLE 2

*Parameters used in the model calculations**

	Units	site C	site M	site S
Fixed Sediment Parameters				
Sedimentation rate	cm/kyr	1.0 (*2,5*)	1.0 (*2*)	0.4 (*2*)
Sediment density	g_{ds}/cm^3_{ts}	2.65 (*2*)	2.65 (*2*)	2.65 (*2*)
Porosity	cm^3_{pw}/cm^3_{ts}	0.7 (*2*)	0.8	0.7 (*2*)
Mn Oxides Flux	$mmol/m^2/yr$	0.1 (*2,3*)	0.3 (*2,3*)	0.1 (*2,3*)
Fe Oxides Flux	$mmol\ m^2/yr$	0.5	0.59	0.5
Bottom Water Conc.:				
Oxygen	μM	167.0 (*5*)	110.0 (*5*)	167.0 (*5*)
Nitrate	μM	36.6 (*2*)	40 (*6*)	36 (*2*)
Manganese	nM	6.0	6.0 (*7*)	6.0
Iron	nM	6.0	6.0	6.0
Adjustable Rate Constants				
OM Oxid Rates				
by Oxygen (k_{ar})	1/yr	2.3×10^{-3}	6.8×10^{-3}	1.3×10^{-3}
by Nitrate (k_{dn})	1/yr	6×10^{-4}	1.2×10^{-3}	—
by Mn Oxides (k_{red})	$g_{ds}/mmol/yr$	1.3×10^{-4}	5.2×10^{-4}	—
by Fe Oxides (k_{fred})	$g_{ds}/mmol/yr$	6.5×10^{-4}	10×10^{-4}	—
Mn Oxid. Rate				
by Oxygen (k_{mox})	1/yr	50	50	—
Fe Oxid. Rates				
by Oxygen (k_{fox})	$l_{pw}/mmol/yr$	1×10^6	1×10^6	—
by MnO_2 (k_{fm})	$g_{ds}/mmol/yr$	100	100	—
by Nitrate (k_{fn})	$l_{pw}/mmol/yr$	150	150	—
NH_3 Oxid. Rates				
by Oxygen (k_{ao})	$l_{pw}/mmol/yr$	20	20	—
by Nitrate (k_{an})	$l_{pw}/mmol/yr$	10	10	—
Free Ion Diffusion Coefficients (all three sites): (*8*)				
Oxygen (D_o)	cm^2/yr	3.73×10^2		
Nitrate (D_n)	cm^2/yr	3.32×10^2		
Manganese (D_m)	cm^2/yr	1.06×10^2		
Iron (D_f)	cm^2/yr	1.17×10^2		
Ammonia (D_a)	cm^2/yr	3.34×10^2		

* Numbers in parentheses refer to the references noted below.

(*1*) Kadko (1981)
(*2*) Jahnke and others (1982b)
(*3*) Kalhorn and Emerson (1984)
(*4*) Emerson and others (1985)
(*5*) Cochran (1985)
(*6*) Heggie, Kahn, and Fischer (1986)
(*7*) Price (1988)
(*8*) Li and Gregory (1974)

decreases. The burial of organic matter is not affected here, in that the sum of the depth-integrated rates of oxic and sub-oxic remineralization is constant and equal to the flux of metabolizable organic matter to the sediments. These changes therefore simply "repartition" organic matter oxidation, and only the non-metabolizable fraction of organic matter is buried in the sediments.

The effects of sediment porosity on sediment properties can also be seen in figure 4. Increasing porosity from 0.7 to 0.75 has a major effect on solid phase Mn concentrations in the oxic zone (which decrease by a factor of ≈ 2; fig. 4D), along with resulting changes in the dissolved Mn

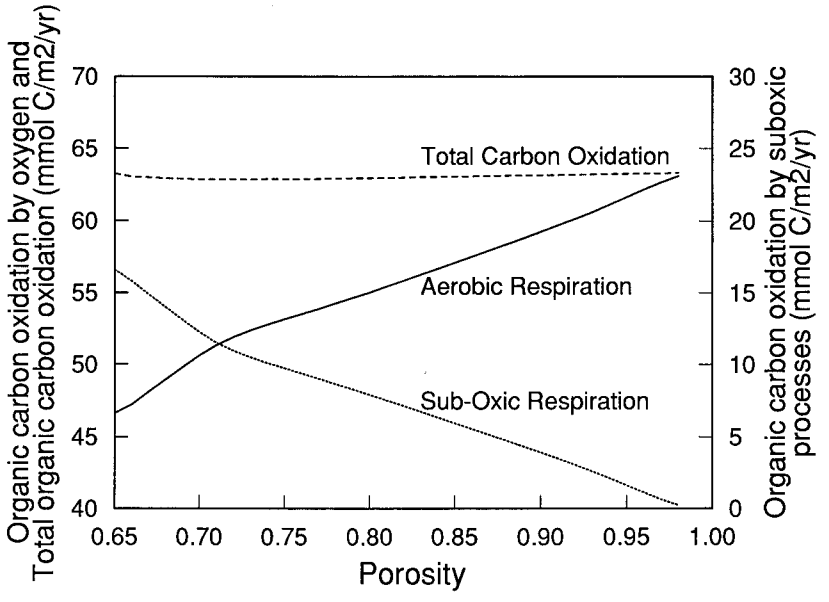

Fig. 3. The effect of increasing sediment porosity on model determined, depth-integrated rates of organic carbon oxidation by oxic (oxygen; solid line) and sub-oxic (nitrate, manganese, and iron; dotted line) processes. The dashed line represents the integrated rate of the total organic carbon oxidation. With the exception of sediment porosity and the organic carbon flux (63.3 mmol/m^2/yr) all other parameter used in the calculations are listed in table 2 for site C.

concentrations in the sub-oxic zone (which decrease by a factor of > 3; fig. 4E). This change in porosity also has a significant affect on the particulate and pore water Fe profiles (fig. 4F and G), and the oxygen penetration depth increases as porosity increases (fig. 4B). While increasing the sediment porosity from 0.7 to 0.75 significantly affects many sedimentary profiles, profiles very similar to the original ($\phi = 0.7$) profiles can also be obtained for $\phi = 0.75$ by adjusting the bioturbation coefficient and the organic matter oxidation rate constants (fig. 4). The fact that the magnitudes of these constants are very poorly constrained suggests to us that, at this stage, the use of depth-dependent porosity in the model may be unnecessary. However, we also recognize that the next step in the development of models such as this one is to include depth-dependent porosity.

The results in figure 5 show the influence of bioturbation on the occurrence of oxic and sub-oxic respiration in sediments. With increasing bioturbation, greater amounts of organic matter are transported deeper into the sediment, therefore decreasing aerobic respiration (fig. 5A) and increasing sub-oxic respiration (fig. 5B). These results are consistent with the model results of Aller (1990). However, increasing the bioturbation

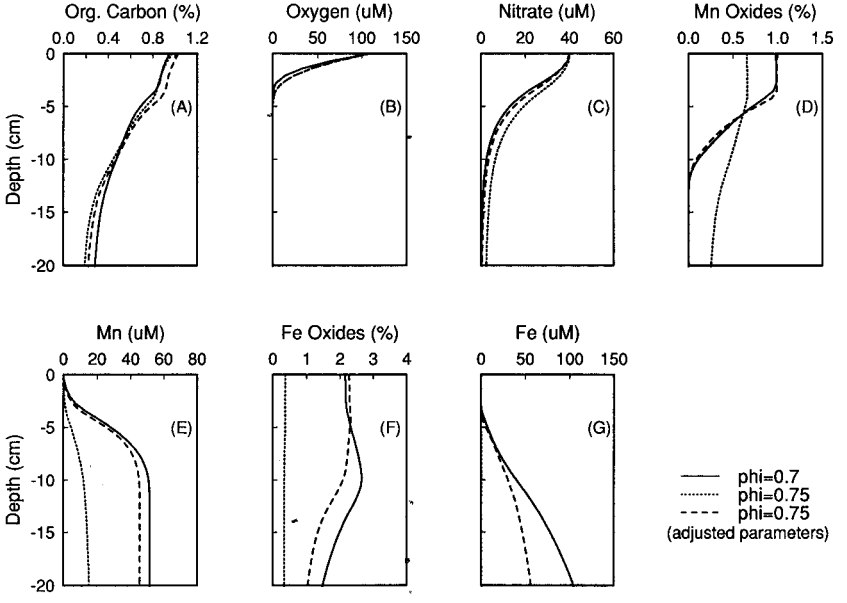

Fig. 4. The effect of porosity on model determined, depth distribution of organic carbon, oxygen, nitrate, manganese, and iron in the sediments. Solid and dotted lines represent concentration profiles determined by the model with ϕ values of 0.7 and 0.75 respectively. The dashed lines are the profiles obtained with $\phi = 0.75$ in which the organic carbon oxidation rate constants and bioturbation coefficient have been varied to obtain profile similar to the original $\phi = 0.7$ curves (k_{ox} has been adjusted from = 0.0068 yr^{-1} to 0.006 yr^{-1}, k_{dn} from 0.0012 yr^{-1} to 0.0015 yr^{-1}, k_{red} from 5.2×10^{-4} g_{ds}/mmol/yr to 20.8×10^{-4} g_{ds}/mmol/yr, k_{fred} from 10×10^{-4} g_{ds}/mmol/yr to 24×10^{-4} g_{ds}/mmol/yr, and K_b^o from 214 cm^2/kyr to 252 cm^2/kyr). With the exception of porosity, the rate constants discussed above, and the organic carbon flux (85 mmol/m^2/yr), all other parameter used in the calculations are listed in table 2 for site M.

coefficient does not affect organic matter burial, since this increase again only "repartitions" organic matter oxidation, and the sum of the depth-integrated rates of oxic and sub-oxic remineralization remains constant. Increasing bioturbation also does not significantly change the depth of the sediment redox boundary (results not shown here), since a decrease in oxygen consumption by aerobic respiration is apparently balanced by an increase in oxygen consumption by pore water Mn and Fe oxidation. Our model results are similar to those of Jahnke and others (1982b) which show that changes in sediment mixing by a factor of two had insignificant effects on pore water oxygen and nitrate profiles.

The effects of changes in sedimentation rates on sediment processes are shown in figures 6 and 7. Increasing sedimentation rates decrease oxygen consumption by organic matter oxidation (fig. 6A) and increases carbon oxidation by sub-oxic diagenesis until all sub-oxic electron acceptors have been consumed in the sediments (fig. 6B-E). As a result, burial

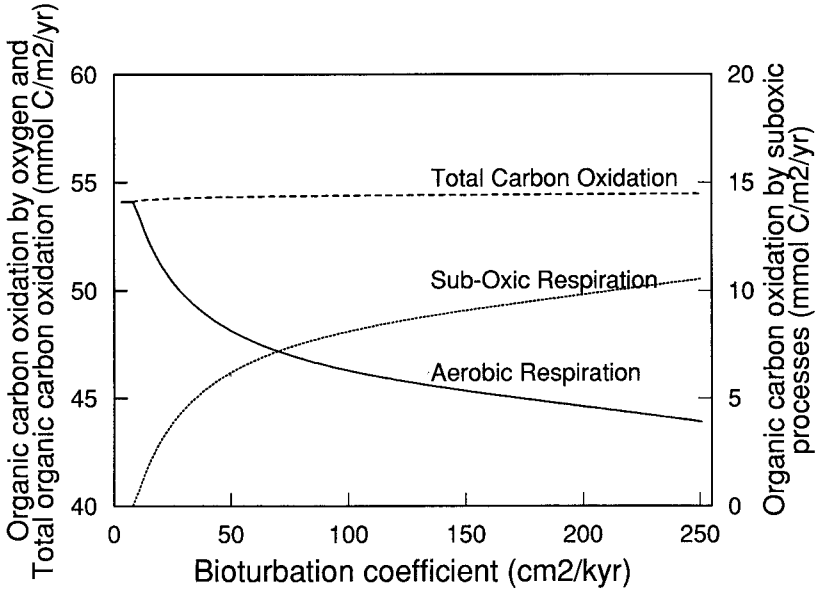

Fig. 5. The effect of increasing the surface bioturbation coefficient (K_b^0) on model determined, depth integrated rates of organic carbon oxidation by oxic (oxygen) and sub-oxic (nitrate, manganese, and iron) processes. The dashed line represents the integrated rate of the total organic carbon oxidation. With the exception of the bioturbation coefficients and the organic carbon flux (62.5 mmol/m^2/yr) all other parameters used in the calculations are listed in table 2 for site C.

of reactive organic matter eventually occurs and then increases with increasing sedimentation rates (fig. 6F). Denitrification first increases and then decreases as sedimentation rates increase (fig. 6C). As sedimentation rates increase, the nitrate flux to the overlying bottom water decreases due to a decrease in the pore water nitrate gradient at the sediment surface (see fig. 7C); thus more nitrate is available for organic matter oxidation by denitrification. However, since aerobic respiration decreases with increasing sedimentation rates (fig. 6A), nitrate production from nitrification also decreases, and less nitrate is, therefore, available for denitrification. The balance between these two opposing trends thus leads to the observations in figure 6C.

The effect of changes in the sedimentation rate on the occurrence of Mn reduction is somewhat complex and is shown in figure 6D. As sedimentation rates increase, organic matter oxidation by Mn reduction first decreases as denitrification increases (fig. 6C and D). When denitrification begins to decrease with increasing sedimentation rates, organic matter oxidation by Mn reduction then increases until net Fe reduction occurs. Once net Fe reduction in organic matter oxidation begins, organic matter oxidation by Mn reduction shows a slight decrease, as a

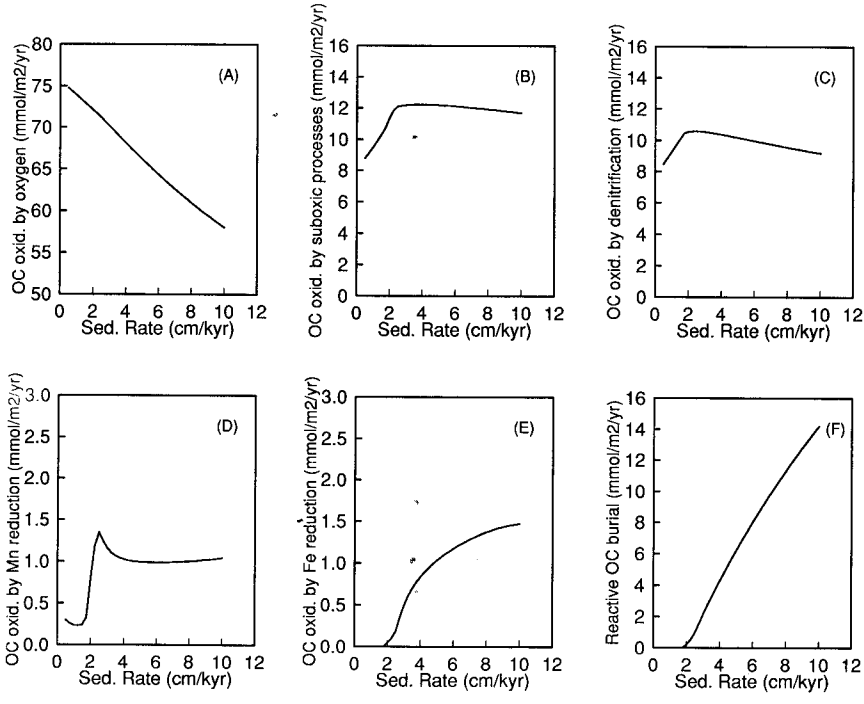

Fig. 6. The effect of increasing the sedimentation rate on model determined, depth-integrated rates of organic carbon oxidation by oxic (oxygen) and sub-oxic (nitrate, manganese, and iron) processes, and the burial of reactive (metabolizable) organic carbon burial rate. With the exception of sedimentation rates and the organic carbon flux (55 mmol/m^2/yr) all other parameter used in the calculations are listed in table 2 for site C.

result of the increasing importance of Mn reduction coupled to Fe^{2+} oxidation.

The model results in figure 7 suggest that variations in the sedimentation rate by a factor of two over a typical range for pelagic sediments (1.0-2.0 cm/kyr) have a minor effect on the pore water profiles of oxygen and nitrate (fig. 7A, B, and C), supporting the results of Jahnke and others (1982b) and Rabouille and Gaillard (1991a). However, these changes do have significant effects on the pore water and solid phase Mn and Fe profiles (fig. 7D-G).

VII. MN CYCLING AND THE FORMATION OF A MN-PEAK IN SEDIMENTS

The results in figure 8A, B, and C and table 3 illustrate the effect of increasing the organic carbon flux to the sediments on the distribution of Mn in the sediments. The concentration of Mn in the zone of maximum bioturbation (C_s), the depth integrated Mn oxidation rate (DIMOR), and the fraction of sub-oxic metabolism accounted for by Mn reduction (R_m)

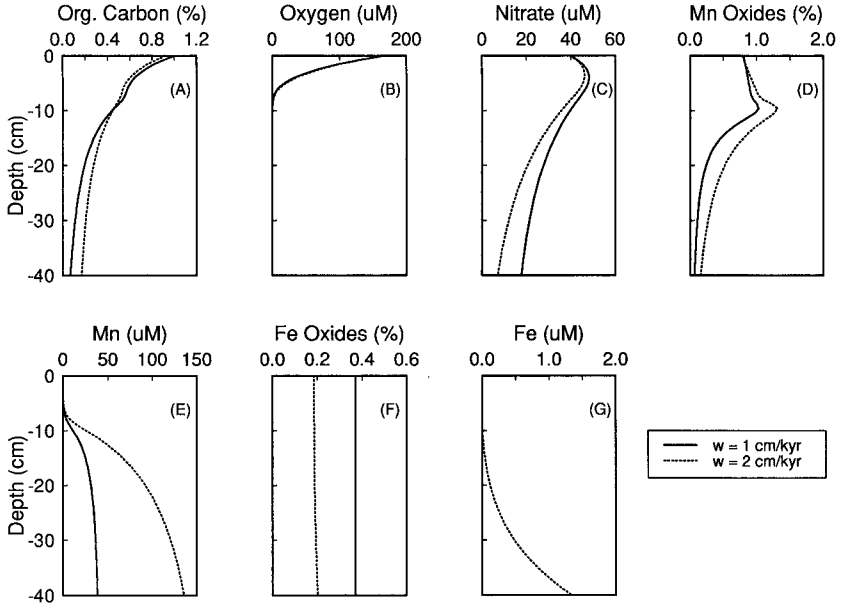

Fig. 7. The effect of the sedimentation rate on model determined, depth distributions of organic carbon, oxygen, nitrate, manganese, and iron in the sediments. Solid and dotted lines represent concentration profiles determined at ω = 1.0 and 2.0 cm/kyr respectively. With the exception of sedimentation rates and the organic carbon flux (55 mmol/m^2/yr) all other parameter used in the calculations are listed in table 2 for site C.

all increase with increasing organic carbon flux. We have also calculated the number of times Mn is recycled internally in diagenetic processes (r) before it either gets permanently buried in the sediments or escapes as a pore water Mn flux to the overlying bottom water (compare Eppley and Peterson, 1979). The results in table 3 show that r also increases with increasing organic carbon flux. Taken together, these observations indicate the important effects that internal Mn redox cycling has on sediment characteristics. First, an increase in Mn recycling leads to concentrations of Mn in the oxic zone well above those which would occur in totally oxic sediments (see R_C in table 3). Second, the increase in the internal recycling of Mn increases the importance of Mn in early diagenetic processes in sediments (see R_m in table 3).

The internal redox recycling of Mn in sediments leads either to the formation of a Mn-peak near the sediment redox boundary or to surficial Mn-rich oxic sediments. The formation of a Mn-peak occurs when pore water Mn concentrations are low in the sub-oxic zone and the redox boundary is relatively deep, due to the low organic carbon flux to the sediment (fig. 8A). Mn oxidation near the sediment redox boundary dominates over the upward diffusion, and a large fraction (> 80 percent)

TABLE 3

Effects of variation in organic carbon (OC) flux on the internal redox cycling and concentration of manganese in sediments

OC flux*	C_s**	$R_C = C_s/C_o$***	DIMOR*,†	r††	R_m†††
42	0.86	1.1	0.11	0.8	6.4%
50	5.98	7.5	1.48	28.2	24.9%
65	28.56	35.7	7.43	67.3	48.2%

* OC fluxes and DIMOR are in mmol/m^2/yr. With the exception of the organic carbon fluxes all other parameters used in these calculations are listed in Table 2 for site C.

** C_s is the depth-integrated concentration of manganese (mol/m^2) in the zone of maximum bioturbation (upper 8 cm).

*** C_o is the depth-integrated concentration of manganese (mol/m^2) in upper 8 cm of completely oxic sediments (with no sub-oxic diagenetic processes). For these sediments where ω = 1 cm/kyr, C_o = 0.8 mol/m^2.

† DIMOR is the depth-integrated manganese oxidation rate in the sediments.

†† r is the number of times manganese is recycled internally before it gets permanently buried in sediments or escapes as a pore water manganese flux to the overlying waters (c.f., Eppley and Peterson, 1979). The parameter r is given by $(1 - f)/f$, where f is the particulate Mn flux at the sediment-water interface divided by DIMOR.

††† R_m is the percentage of depth-integrated organic carbon oxidation by sub-oxic processes that occurs by manganese reduction.

of the manganese oxidation occurs at depths in the sediments where the bioturbation coefficient is < 10 cm^2/kyr (fig. 8D). This effectively leads to a separation of the zones of Mn oxidation and bioturbation, and a Mn peak forms below the zone of bioturbation near the sediment redox boundary (fig. 8A and D). In contrast, when upward diffusion of pore water Mn dominates over oxidation near the sediment redox boundary, a significant fraction ($\approx$60 percent) of the manganese oxidation occurs in the zone of bioturbation (fig. 8F). This occurs when pore water Mn concentrations are high in the sub-oxic zone, and the sediment redox boundary is relatively shallow, due to the relatively high organic carbon flux to the sediments. These conditions then lead to a high concentration of solid phase Mn in the oxic zone and the lack of a distinct Mn-peak near the redox boundary in the sediments (fig. 8C).

VIII. APPLICATION OF THE MODEL TO DATA FROM THE MANOP PROGRAM

Further to test our model we have used it to examine sediment data from three contrasting sites studied in the MANOP program (sites M, S, and C). We have chosen to examine these sites in part because of the large amount of information collected on their geochemistry (Goloway and Bender, 1982; Jahnke and others, 1982b; Kadko and Heath, 1984; Kalhorn and Emerson, 1984; Lyle, 1983; Lyle, Heath and Robbins, 1984; Reimers and others, 1984; Cochran, 1985; Dymond and Lyle, 1985; Emerson and others, 1985; Heggie, Kahn, and Fischer, 1986; Murray, 1987, Finney, Lyle, and Heath, 1988; and others). We are also able to compare the results of our calculations with other papers that have quantified organic matter remineralization in these sediments (Bender and Heggie, 1984; Berelson and others, 1990; Emerson and others,

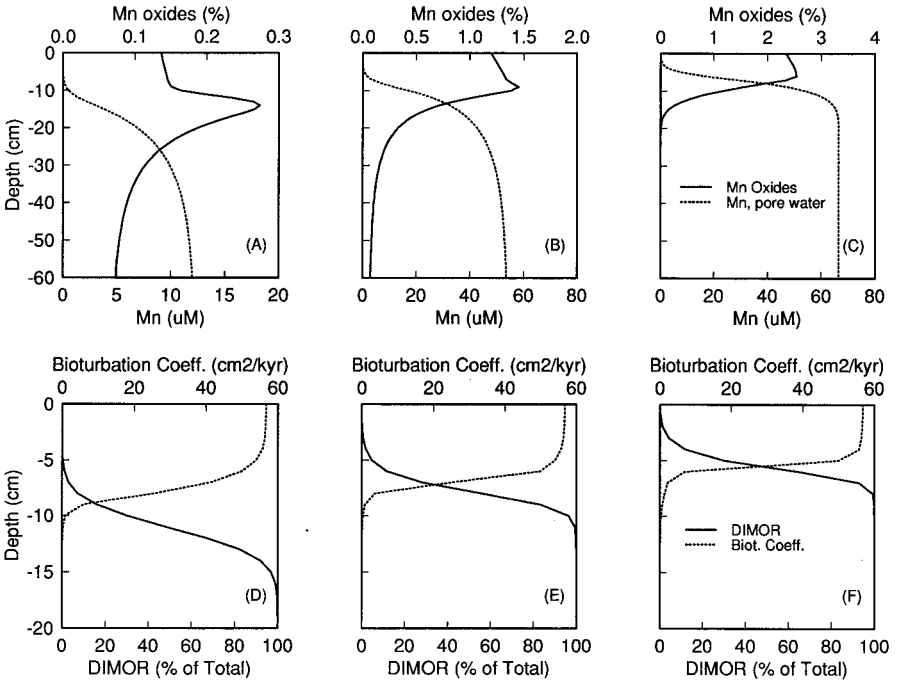

Fig. 8. The effects of increasing the organic carbon flux to the sediments (42, 50, and 65 mmol/m^2/yr in figure 8, A, B, and C, respectively) on pore water and solid phase manganese concentrations in sediments. Figure 8, D, E, and F, show the depth integrated manganese oxidation rates (DIMOR, dotted line) and the bioturbation coefficients (solid line) for the same organic carbon fluxes. With the exception of the organic carbon fluxes all other parameter used in the calculations are listed in table 2 for site C. Note that the same manganese flux is used in all cases.

1985). Additional details on the characteristics of the sites are discussed in the remainder of this section and in the papers cited above. It should also be noted here that in examining the data from these sites, data from "replicate" cores from the same site do not always agree (Emerson and others, 1985; Jahnke and others, 1982b). This most likely results from some degree of spatial heterogenity.

The parameters used in modeling this data are given in tables 2, 4, and 5. For situations where more than one value of a parameter has been cited in the literature, we have chosen the value that best fits the pore water and solid phase data. In using this model to fit the field data we have taken the maximum bioturbation coefficient (K_b^0) to be an adjustable parameter, and the results in table 5 indicate that these "best-fit" K_b^0 values agree well with independent estimates of bioturbation coefficients. The best-fits to the data are shown in figures 9, 10, and 11. Model estimates of the rates of sediment processes and fluxes at the sediment-

water interface are listed in tables 4, 6, and 7 and are also compared with independent estimates of these quantities.

The results of fitting the data from MANOP site M to our model are shown in figure 9. In general, the model results are in reasonably good agreement with the field data. Although detailed pore water oxygen data are not available at this site, the depth of oxygen penetration predicted by our model (4.5 cm) is similar to the value (5 cm) reported by Emerson and others (1985). Model calculations suggest that ≈84 percent of the organic matter is oxidized in these sediments by oxygen and ≈16

TABLE 4

Comparison of estimates of the organic carbon flux at the sediment-water interface of the MANOP sites

Estimated From	site M	site C	site S	Reference
Sediment Carbon Gradient	80-130	70-240	90-500	1
Sediment Trap	120-150	—	17	1
Sediment Trap	—	135 ± 62	47 ± 40	2
O_2 Microelectrode Flux	—	232 ± 14	70 ± 18	3
Benthic Chamber	—	124 ± 18	106 ± 55	4
Pore Water Nitrate Flux	200-218	204	18	5
Pore Water Nitrate Flux	—	47	25	6
This Work	110	47	25	—

All fluxes are in mmol/m^2/yr.
1. Emerson and others (1985)
2. Dymond and Collier (1988)
3. Reimers and others (1984)
4. Berelson and others (1990)
5. Bender and Heggie (1984) and Goloway and Bender (1982)
6. Jahnke and others (1982b)

TABLE 5

Comparison of estimates of the maximum bioturbation coefficients (cm^2/kyr) in surface sediments at MANOP sites

Estimated From	site M	site C	site S	Reference
^{210}Pb profile	158-505	158	<101	1
^{210}Pb profile	—	32	32	2
Model 1	158	151	199	3‡
Model 2	—	32	32	4
Model 3	—	—	25	5
This Work (K_B)	214	52	32	—

1. Cochran (1985)
2. Kadko (1981)
3. Emerson and others (1985)
4. Jahnke and others (1982b)
5. Rabouille and Gaillard (1991a)

‡ For site S this bioturbation coefficient was estimated with ^{137}Cs data, while for sites M and C these coefficients were estimated with ^{210}Pb data (Cochran, 1985). According to Cochran (1985) bioturbation coefficients estimated by ^{137}Cs are 6 to 7 times higher than the coefficients estimated by ^{210}Pb.

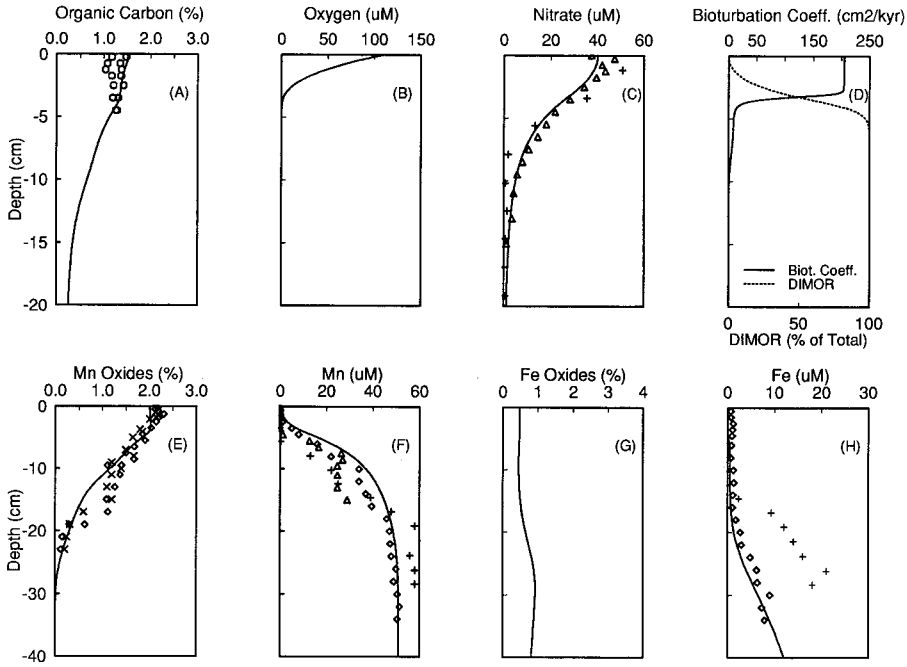

Fig. 9. A comparison between field data from MANOP site M and the best fit to these data determined by the model (a-c; e-h). The depth dependence of the bioturbation coefficient (solid line) and the depth integrated manganese oxidation rate (DIMOR, dotted line) determined by the model are shown in figure 9D. Symbol designation in this figure is as follows: ○ Emerson and others (1985); △ Heggie, Kahn and Fischer (1986); + Klinkhammer (1980); × Kalhorn and Emerson (1984); ◇ Lyle, Heath, and Robbins (1984).

percent is oxidized by sub-oxic diagenetic processes (table 6). Furthermore, the solid phase Mn flux to the sediment-water interface is only 0.3 mmol/m^2/yr (Fischer, 1983; Kalhorn and Emerson, 1984, see table 2), whereas the Mn consumed in the organic matter oxidation is 5.0 mmol/m^2/yr. Such a comparison indicates the importance of the internal redox cycling of Mn in these sediments (Burdige, 1993). Due to the high organic carbon flux to these sediments, the redox boundary at this site is shallow and pore water Mn concentrations are high in the sub-oxic zone, with a steep concentration gradient near the sediment redox boundary. Upward diffusion of dissolved Mn therefore dominates over Mn oxidation near the sediment redox boundary. More than 90 percent of the Mn oxidation occurs in the bioturbated zone of these sediments (fig. 9H), and the oxidized Mn is homogenized by sediment mixing processes, resulting in a high concentration of Mn in the oxic zone of the sediments and the lack of a distinct Mn-peak near the sediment redox boundary. Our calculations also suggest that a large fraction (>90 percent) of the particulate Mn flux to these sediments escapes as a pore water Mn flux,

TABLE 6

*Comparison of depth integrated net organic carbon (OC) oxidation rates**

	This Work	Bender and Heggie (1984)
site C		
Avg. OC flux	47.0	—
OC Oxidation	46.3	204.0
by Oxygen	44.5	200.0
by Nitrate	1.5	3.2
by Manganese	0.3	0.8
by Iron	0.02	—
OC Burial	0.7	2.0
site M		
Avg. OC flux	110.0	130.0
OC Oxidation	109.7	128.3
by Oxygen	92.1	118.0
by Nitrate	15.1	9.0
by Manganese	2.3	1.0
by Iron	0.2	0.1
OC Burial	0.7	4.0
site S		
Avg. OC flux	25.0	18.0
OC Oxidation	24.5	18.0
by Oxygen	24.5	18.0
by Nitrate	0.0	—
by Manganese	0.0	—
by Iron	0.0	—
OC Burial	0.5	0.1

*All depth-integrated rates are in mmol/m^2/yr.

and as a result less than 10 percent of original particulate Mn flux is permanently buried in the sediments. For comparison, Kalhorn and Emerson (1984) calculated that only 30 percent of the particulate Mn flux to these sediments is buried in the sediments. Heath and Lyle (1982) also suggested that only a small fraction of the particulate hydrothermal Mn flux to the sediments is buried at this site, based on the sediment Fe/Mn ratio.

In contrast to site M, the sediments at site S are totally oxic, with no evidence for the occurrence of sub-oxic diagenesis (fig. 10). Aerobic respiration, therefore, accounts for 100 percent of the carbon metabolism in these sediments. Our model results are in good agreement with the field data with the exception of the organic carbon data near the sediment-water interface. This may result from the fact that the sediments at this site are fairly heterogeneous (Emerson and others, 1985; Jahnke and others, 1982b).

Finally, at site C geochemical data and model results in figure 11 provide evidence for the occurrence of both oxic and sub-oxic processes in these sediment (denitrification and Mn reduction only). However, when compared to the model fits to the sites M and S data, there is not good agreement at site C between model results and some sediment profiles. Due to low pore water Mn concentrations in the sub-oxic zone, Mn oxidation dominates over diffusion near the sediment redox bound-

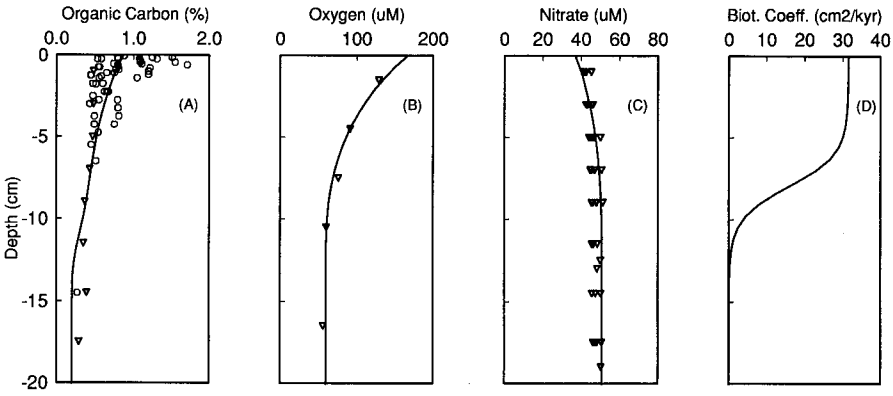

Fig. 10. A comparison between field data from MANOP site S and the best fit to these data determined by the model. No sub-oxic processes occur at this site, hence manganese and iron profiles are not shown. Symbol designation is the same as in figure 9, with the addition of: ▽ Jahnke and others (1982).

ary. A significant fraction, ≈80 percent, of the Mn oxidation therefore occurs below the zone of bioturbation. While this then leads to a Mn-peak in the sediments at 11 to 12 cm, we also observed that a deeper Mn peak can form at a depth of 14 to 15 cm, if we increase the value of K_{ox} (oxygen half saturation constant for OM oxidation) from 3.1 to 6.0 μM (see fig. 11D). Based on pore water Mn profiles, Emerson and others (1985) estimated that oxygen concentrations go to zero at a depth of 9.5 cm in these sediments (slightly shallower than the model result shown in fig. 11B), and, therefore, a Mn-peak should be seen at ≈9.5 cm depth. Murray (1987) reported a Mn-peak in these sediments near 17 to 18 cm (see fig. 11D). Finally, oxygen microelectrode profiles at this site (Reimers and others, 1984) show an oxygen penetration depth of ≈2 cm, suggesting that only upper 2 cm of these sediments should be Mn rich. These apparent discrepancies may be due in part to a comparison of data from different cores collected at this site (spatial heterogenity), since Jahnke and others (1982b) have also reported large variations in Mn depth profiles (by as much as a factors of 2-3) in different sediment cores from site C.

Alternatively, this lack of agreement between modeled and observed Mn profiles and the oxygen penetration depth may be due to non-steady state diagenetic processes in these sediments. Several lines of evidence support this suggestion. The first is that our model results and pore water Mn profiles predict a sediment redox boundary of 9 to 10 cm, whereas solid phase Mn profiles predict a slightly deeper redox boundary (17-18 cm, see fig. 11). This suggests the occurrence of a net upward shift in the depth of the sediment redox boundary at some point in the recent past (Burdige, 1993), since in general pore water Mn and oxygen profiles adjust more rapidly to such changes in sediment redox conditions than

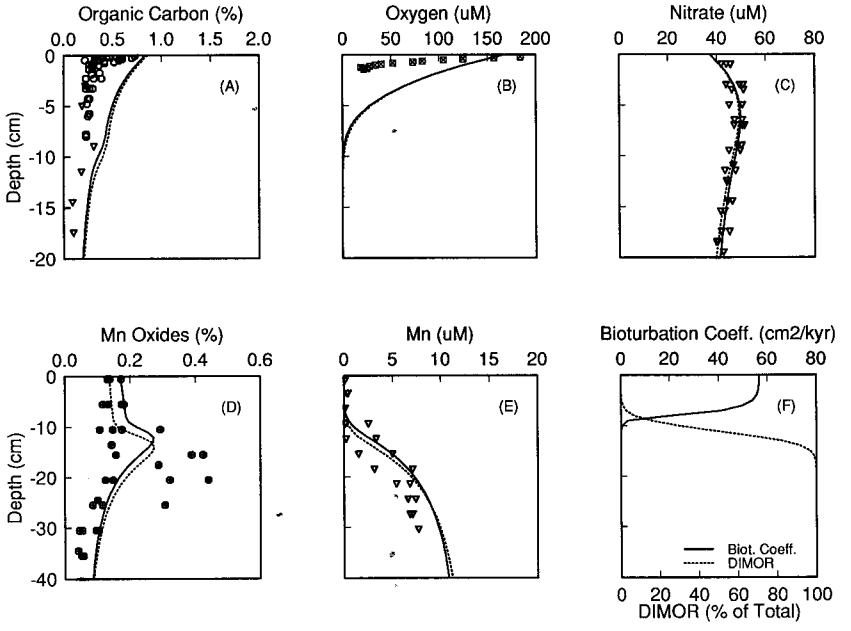

Fig. 11. A comparison between field data from MANOP site C and the best fit to these data determined by the model (a-e). Solid and dotted lines in figure 11, A through E, are model concentration profiles determined with K_{ox} values of 3.1 and 6.0 μM respectively. The depth dependence of the bioturbation coefficient (solid line) and the depth-integrated manganese oxidation rate (DIMOR, dotted line) at K_{ox} = 6.0 μM determined by the model are shown in figure 11F. Besides oxygen data which are from Reimers and others (1984), symbol designation is the same as in figure 9, with the addition of: ⊗ Murray (1987); ☒ Reimers and others (1984).

do solid phase Mn profiles (Froelich and others, 1979; Price, 1988; Pedersen, Vogel, and Southon, 1986; Burdige, 1993; Dhakar and Burdige, 1994). Secondly, organic carbon profiles at this site show a sub-surface maxima between 30 to 50 cm followed by a sharp exponential-like decrease below this sub-surface maxima (Murray, 1987), suggesting possible changes with time in the flux of organic carbon to these sediments. Finally, gravity core results indicate that the actual zone of Mn reduction may occur below 100 cm (Jahnke and others, 1982b), and that there is a considerable spatial separation in these sediments between this deeper zone of Mn reduction and the zone of Mn oxidation above 10 cm. Overall, these observations suggest the possibility of some spatial separation at site C between a zone of organic matter remineralization near the sediment-water interface and a deeper zone of remineralization below ≈ 30 to 50 cm. If this is the case, the region between these two zones may represent a non-reactive zone in which diffusion controls the concentrations of pore water constituents. The occurrence of such phenomena in

TABLE 7

Comparison of fluxes at the sediment-water interface

Estimated From	Oxygen*	Nitrate*	Reference
site S			
Model 1	32.9 ± 3.7	−3.7 ± 0.7	1
Model 2	18.3 ± 7.3	−2.2 ± 0.7	2
O_2 Microelectrode	91.3 ± 21.9		3
Benthic Lander	124 ± 62	−9.7 ± 5.1	4
This Work	31.8	−3.6	—
site C			
Model 1	62.1 ± 11	−6.9 ± 0.4	1
Model 2	197.1 ± 91.3	−23.4 ± 12.8	2
O_2 Microelectrode	303 ± 18.3		3
Benthic Lander	142.3 ± 29.2	−9.1 ± 4.4	4
Whole Core Squeezer	124.6	−14.6	4
This Work	58.4	−5.3	—
site M			
Model 2	260-284	−15.18	2
This Work	121.6	−6.5	—

* All fluxes are in mmol/m^2/yr, and negative fluxes are out of the sediments.
1. Jahnke and others (1982b)
2. Bender and Heggie (1984) and Goloway and Bender (1982)
3. Reimers and others (1984)
4. Berelson and others (1990)

other marine sediments has been discussed by several workers (Goloway and Bender, 1982; Wilson and others, 1985; Jahnke and others, 1989) and appears to be related to non-steady state diagenetic processes in these sediments (also see Burdige, 1993). Unfortunately, this scenario can not also explain the discrepancy between a sediment redox boundary at either 9 to 10 cm or 17 to 18 cm and the very shallow (2 cm) oxygen penetration depth based on the oxygen microelectrode data of Reimers and others (1984). We note that also Emerson and others (1985) were unable to reconcile this oxygen data with other field data from site C sediments.

For all these sites a comparison of the model "best fit" fluxes of organic carbon to the sediment surface agrees well with some of the other independent estimates of these quantities (table 4). However, given the large ranges in the estimates in this table, it is difficult to interpret this "agreement." Benthic oxygen and nitrate fluxes calculated with our model show a slightly better agreement with independent estimates of these quantities (table 7). Finally a comparison of depth-integrated organic matter oxidation rates estimated by this model and by Bender and Heggie (1984) is given in table 6. The rates of organic matter oxidation for site C estimated by Bender and Heggie (1984) are higher by a factor of 4 than the rates estimated by this model. However Bender and Heggie (1984) note that they may have overestimated rates in site C sediments based on an assumption of variable core top loss in the sediment cores they examined. In addition, they also note that they may

have underestimated rates at site S by neglecting core top loss. These suggestions are consistent with the results in table 6.

IX. CONCLUSIONS

A steady state, coupled, non-linear model has been presented for early diagenetic processes in pelagic sediments. The model includes diagenetic processes that occur in oxic and sub-oxic sediments and also uses a new approach to quantify the depth dependence of sediment mixing. Model results show that an increase in sedimentation rates and sediment mixing increases organic matter oxidation by sub-oxic processes, whereas an increase in porosity increases organic matter oxidation by oxic processes. An increase in the organic matter flux to the sediment surface increases the internal redox cycling of Mn and has significant effects on the occurrence of sub-oxic diagenetic processes.

The distribution of Mn in pelagic sediments and the formation of a Mn-peak near the redox boundary of some bioturbated sediments can be explained by assuming that the depth of the sediment mixed layer is partially a function of the pore water oxygen concentration. In sediments where the organic matter flux is large and the sediment redox boundary is shallow (<5 cm), upward diffusion of pore water manganese into overlying oxic sediments dominates over manganese oxidation near the sediment redox boundary, and Mn-rich oxic sediments are formed. In contrast, in sediments where the organic matter flux is low and the sediment redox boundary is deep (>10 cm), manganese oxidation near the sediment redox boundary dominates over pore water manganese diffusion into the overlying oxic sediments. In this case, a distinct Mn-peak forms near the sediment redox boundary.

Good agreement of model results with field data from the MANOP sites suggests that this linkage between sediment mixing and pore water oxygen concentrations better describes the depth dependence of sediment mixing than that used in other models. However we also recognize that further laboratory and field studies on the factors controlling the depth-dependence of sediment mixing are needed to verify our assumption of oxygen-dependent bioturbation. The discrepancy at site C between model and observed profiles may in part be due to the occurrence of non-steady state processes in these sediments. The data from this site may therefore be better explained by a non-steady state version of this model which we are currently developing.

ACKNOWLEDGMENTS

We thank an anonymous reviewer and the following people for reading earlier versions of this manuscript and for providing us with many useful suggestions: Steve Skrabal, David Archer, Jack Middelburg, and Bernard Boudreau. We especially thank John Klinck for his advice and guidance in the development of the numerical solution to the model equations. We also thank The Center for Coastal Physical Oceanography at Old Dominion University for providing computer facilities for some of

the work described here. Acknowledgment is made to the Donors of The Petroleum Research Fund, administered by the American Chemical Society, for the support of this research.

APPENDIX 1

Organic Carbonate

$$0 = -\frac{\partial}{\partial x}\left[-K_b\frac{\partial G}{\partial x} + \omega G\right] - \frac{l_a k_{ar} OxG}{K_{ox} + Ox} - \frac{l_d k_{dn} NGf_x}{K_n + N} - l_m k_{red} GM_s f_x - l_f k_{fred} GF_s f_f$$

Manganese Solid Phase

$$0 = -\frac{\partial}{\partial x}\left[-K_b\frac{\partial M_s}{\partial x} + \omega M_s\right] + \frac{M_p}{F}\frac{Ox\,k_{mox}}{K_{mox} + Ox} - k_{red} GM_s f_x - \frac{1}{F} l_{fm} k_{fm} F_e M_s$$

Manganese Dissolved Phase

$$0 = -\frac{\partial}{\partial x}\left[-(D_m + K_b)\frac{\partial M_p}{\partial x} + \omega M_p\right] - \frac{M_p Ox\,k_{mox}}{K_{mox} + Ox} + Fk_{red} GM_s f_x + l_{fm} k_{fm} F_e M_s$$

Iron Solid Phase

$$0 = -\frac{\partial}{\partial x}\left[-K_b\frac{\partial F_s}{\partial x} + \omega F_s\right] + \frac{1}{F} k_{fox} OxF_e - k_{fred} GF_s f_f + \frac{1}{F} k_{fm} F_e M_s + \frac{1}{F} k_{fn} NF_e$$

Iron Dissolved Phase

$$0 = -\frac{\partial}{\partial x}\left[-(D_f + K_b)\frac{\partial F_e}{\partial x} + \omega F_e\right] - k_{fox} OxF_e + Fk_{fred} GF_s f_f - k_{fm} F_e M_s - k_{fn} NF_e$$

Oxygen Dissolved Phase

$$0 = -\frac{\partial}{\partial x}\left[-(D_o + K_b)\frac{\partial Ox}{\partial x} + \omega Ox\right] - \frac{l_{mox} M_p Ox\,K_{mox}}{K_{mox} + Ox} - \frac{Fk_{ar} OxG}{K_{ox} + Ox} - l_{fox} k_{fox} OxF_e - l_{on} k_{ao} A_m Ox$$

Nitrate Dissolved Phase

$$0 = -\frac{\partial}{\partial x}\left[-(D_n + K_b)\frac{\partial N}{\partial x} + \omega N\right] - \frac{Fk_{dn} NGf_x}{K_n + N} - k_{an} A_m N - k_{fn} NF_e + k_{ao} A_m Ox + \frac{l_{an} Fk_{ar} OxG}{K_{ox} + Ox}$$

Ammonia Dissolved Phase

$$0 = -\frac{1}{1+K}\frac{\partial}{\partial x}\left[-(D_a + K_b)\frac{\partial A_m}{\partial x} + \omega A_m\right] + \frac{1}{1+K}\left[l_{af} k_{fred} \mathrm{GF_s f_f} - k_{ao} A_m Ox\right] - \frac{1}{1+K}\left[l_n k_{an} A_m N\right]$$

Where:

t = time (yr)
x = depth (cm)
ω = sedimentation (advection) rate (cm/yr)
G = organic carbon concentration (mmol g_{ds}^{-1})
M_s = particulate manganese concentration (mmol g_{ds}^{-1})
F_s = particulate iron concentration (mmol g_{ds}^{-1})
M_p = pore water manganese concentration (mM)

F_e = pore water iron concentration (mM)
Ox = pore water oxygen concentration (mM)
N = pore water nitrate concentration (mM)
D_m = diffusion coefficient for manganese in the sediment ($cm^2\ yr^{-1}$)
D_f = diffusion coefficient for iron in the sediment ($cm^2\ yr^{-1}$)
D_o = diffusion coefficient for oxygen in the sediment ($cm^2\ yr^{-1}$)
D_n = diffusion coefficient for nitrate in the sediment ($cm^2\ yr^{-1}$)
D_a = diffusion coefficient for ammonia in the sediment ($cm^2\ yr^{-1}$)
K_b = bioturbation coefficient ($cm^2\ yr^{-1}$)
k_{ox} = rate constant for OM oxidation by oxygen (yr^{-1})
k_{dn} = rate constant for OM oxidation by nitrate (yr^{-1})
k_{mred} = rate constant for OM oxidation by manganese ($g_{ds}mmol^{-1}yr^{-1}$)
k_{fred} = rate constant for OM oxidation by iron ($g_{ds}mmol^{-1}yr^{-1}$)
k_{ao} = rate constant for ammonia oxidation by oxygen (yr^{-1})
k_{mox} = rate constant for manganese oxidation by oxygen (yr^{-1})
k_{fox} = rate constant for iron oxidation by oxygen ($l_{pw}mmol^{-1}yr^{-1}$)
k_{fm} = rate constant for iron oxidation by manganese (Mn^{4+}) ($g_{ds}mmol^{-1}yr^{-1}$)
k_{fn} = rate constant for iron oxidation by nitrate ($l_{pw}mmol^{-1}yr^{-1}$)
K_{ox} = oxygen half saturation constant for OM oxidation (mM)
K_n = nitrate half saturation constant for OM oxidation (mM)
K = dimensionless linear adsorption coefficient for NH_4^+
l_o = moles of organic carbon oxidized per mole of O_2 consumed
l_d = moles of carbon oxidized per mole of nitrate consumed
l_m = moles of carbon oxidized per mole of manganese oxides reduced
l_f = moles of carbon oxidized per mole of iron oxides reduced
l_n = moles of NH_4^+ consumed per mole of nitrate consumed
l_{mox} = moles of O_2 consumed per mole of Mn^{2+} oxidized
l_{fox} = moles of O_2 consumed per mole of Fe^{2+} oxidized
l_{fm} = moles of manganese reduced per mole of iron oxidized
l_{an} = moles of NO_3^- produced per mole of organic carbon oxidized by O_2
l_{af} = moles of NH_4^+ produced per mole of organic carbon oxidized by Fe^{3+}
l_{on} = the moles of O_2 consumed per mole of NH_3 oxidized
F = the units conversion factor ($g_{ds}\ l_{pw}^{-1}$) = $(1 - \phi)/\phi * \rho * 1000$
f_x = inhibition factor for OM oxidation by Mn^{4+}, NO_3^-
f_f = inhibition factor for OM oxidation by Fe^{3+}

Note that the l values are stoichiometric coefficients based on the C:N:P ratio of the organic matter undergoing remineralization (see table 1) and the stoichiometric coefficients in reactions (2) to (11) in table 1.

Appendix 2

As discussed in the text, the numerical approximation of each differential equation leads to a set of n equations of the form:

$$0 = b_i C_{i-1} + a_i C_i + c_i C_{i+1} \qquad (A\text{-}1)$$

(Note that eq. (*A*-1) is identical to eq. (10) in the text). For pore waters, the upper boundary condition ($x = 0$, $C = C_o$ [bottom water concentration]) allows the first equation to be re-written as:

$$a_1 C_1 + c_1 C_2 = -b_1 C_0 \qquad (A\text{-}2)$$

The numerical approximation of the lower boundary condition ($x \to \infty\ \partial C/\partial x = 0$) implies that $C_{n+1} - C_{n-1}/2\Delta x = 0$, or $C_{n+1} = C_{n-1}$. Therefore the last (n^{th}) equation is re-written as:

$$(b_n + c_n)C_{n-1} + a_nC_n = 0 \tag{A-3}$$

For solid phase constituents, the upper flux boundary condition implies that:

$$F_c = \rho(1 - \phi)\left(-K_b \frac{\partial C}{\partial x} + \omega C\right)_{x=o} \tag{A-4}$$

or

$$\frac{F_c}{\rho(1 - \phi)} = -\frac{K_b^0}{\Delta x}(C_1 - C_o) + \omega C_o \tag{A-5}$$

If we define $f_3 = F_c/\rho(1 - \phi)$ and $f_2 = Kb^o/\Delta x$, then

$$C_o = \frac{f_3 + f_2C_1}{f_2 + \omega} \tag{A-6}$$

and the first equation can be re-written as:

$$\left[a_1 + \frac{b_1f_2}{f_2 + \omega}\right] C_1 + c_1C_2 = -\frac{b_1f_3}{f_2 + \omega} \tag{A-7}$$

Since solid phase components have the same lower boundary condition as pore waters, eq. (*A*-3) also describes the last (n^{th}) equation for solid phase constituents.

References

Aller, R. C. 1982, The effects of macrobenthos on chemical properties of marine sediment and overlying water, *in* McCall, P. L., and Tevsez, M. J., editors, Animal-Sediment Relations, The Biogenic Alterations of Sediments: New York, Plenum Press, p. 53–102.

———— 1990. Bioturbation and Mn cycling in hemipelagic sediments: Philosophical Transactions of the Royal Society of London, v. A 331, p. 51–68.

———— 1994, Bioturbation and remineralization of sedimentary organic matter: effects of redox oscillation. Chemical Geology, v. 114, p. 331–345.

Aller, R. C., and Yingst, J. Y., 1985, Effects of the marine deposit-feeders *Heteromastus filiformii* (polychaeta), *Macoma balthica* (Bivalvia), and *Tellina texana* (Bivalvia) on averaged sedimentary solute transport, reaction rates and microbial distributions: Journal of Marine Research, v. 43, p. 615–645.

Bender, M. L., and Heggie, D. T. 1984, Fate of organic carbon reaching the sea floor: a status report; Geochimica et Cosmochimica Acta, v. 48, p. 977–986.

Bender, M. L., Jahnke, R. A., Weiss, R., Martin, W., Heggie, D. T., Orchardo, J., and Sowers, T. 1989, Organic carbon oxidation and benthic nitrogen and silica dynamics in San Clemente Basin, a continental borderland site: Geochimica et Cosmochimica Acta, v. 53, p. 685–697.

Berelson, W. M., Hammond, D. E., O'Neill, D., Xu, X-M., Chin, C., and Zukin, J. 1990, Benthic fluxes and pore water studies from sediments of the central equatorial north Pacific: nutrient diagenesis: Geochimica et Cosmochimica Acta, v. 54, p. 3001–3012.

Berger, W. H., and Killingley, J. S., 1982, Box cores from the equatorial Pacific: ^{14}C sedimentation rates and benthic mixing: Marine Geology, v. 45, p. 93–125.

Berner, R. A. 1980, Early Diagenesis, A Theoretical Approach: Princeton, New Jersey, Princeton University Press, p. 241.

Boudreau, B. P. 1984, On the equivalence of nonlocal and radial diffusion models for pore water irrigation. Journal of Marine Research, v. 42, p. 731–735.

———— 1986, Mathematics of tracer mixing in sediments: I. Spatially-dependent, diffusive mixing: American Journal of Science, v. 286, p. 161-198.

———— 1986, Mathematics of tracer mixing in sediments: II. Nonlocal mixing and biological conveyor belt phenomena: American Journal of Science, v. 286, p. 199–238.

———— 1994, Is burial velocity a master parameter for bioturbation?: Geochimica et Cosmochimica Acta, v. 58, p. 1243–1249.

Burdige, D. J., 1993, The biogeochemistry of Mn and Fe reduction in marine sediments: Earth-Science Reviews, v. 35, p. 249–284.
Burdige, D. J., Dhakar, S. P., and Nealson, K. H. 1992, Effects of Mn oxide mineralogy on microbial and chemical Mn reduction: Geomicrobiology Journal, v. 10, p. 27–48.
Burdige, D. J., and Gieskes, J. M., 1983, A pore water / solid phase diagenetic model for Mn in marine sediments: American Journal of Science, v. 283, p. 29–47.
Canfield, D. E., 1993, Organic matter oxidation in marine sediments, *in* Wollast, R., Chou, L., and Mackenzie, F., editors, Interactions of C, N, P and S biogeochemical Cycles, NATO-ARW: Berlin, Springer, p. 333–363.
Cochran, J. K., 1985, Particle mixing rate in sediments of eastern equatorial Pacific: Evidence from ^{210}Pb, $^{239,240}Pu$, ^{137}Cs distributions at MANOP sites; Geochimica et Cosmochimica Acta, v. 49, p. 1195–1210.
Coppedge, M. L., and Balsam, W. L., 1992, Organic carbon distribution in the north Atlantic ocean during the last glacial maximum: Marine Geology, v. 105, p. 37–50.
Crank, J., 1975, The Mathematics of Diffusion: Oxford, Clarendon Press, p. 347.
De Lange, G. J., 1986, Early diagenetic reactions in interbedded pelagic and turbiditic sediments in the Nares abyssal plain (western north Atlantic): Consequences for the composition of sediment and interstitial water: Geochimica et Cosmochimica Acta, v. 50, p. 2543–2561.
Devol, A. H., 1978, Bacterial oxygen uptake kinetics as related to biological processes in oxygen deficient zones of the oceans: Deep Sea Research, v. 25, p. 137–146.
Dhakar, S. P., and Burdige, D. J., 1994, A non-steady state, coupled, non-linear model for early diagenetic processes in pelagic marine sediments (abstract): EOS, v. 75(43), p. 390.
Dymond, J., and Lyle, M., 1985, Flux comparison between sediments and sediment traps in the eastern tropical Pacific: implications for atmospheric CO_2 variations during the Pleistocene: Limnology and Oceanography, v. 30, p. 699-712.
Ehrlich, H. L., 1987, Mn oxide reduction as a form of anaerobic respiration: Geomicrobiology Journal, v. 5, p. 423-431.
Emerson, S., Fisher, K., Reimers, C., and Heggie, D., 1985, Organic carbon dynamics and preservation in deep sea sediments: Deep Sea Research, v. 32, p. 1–21.
Emerson, S., and Hedges, J. I., 1988, Processes controlling the organic carbon content of the open ocean sediments: Paleoceanography, v. 3, p. 621–634.
Emerson, S., Jahnke, R., Bender, M., Froelich, P., Klinkhammer, G., Bowser, C., and Setlock, G., 1980, Early diagenesis in the sediments from equatorial Pacific, 1. Pore water, nutrient and carbonate results: Earth and Planetary Science Letters, v. 49, p. 57–80.
Eppley, R. W., and Peterson, B. J., 1979, Particulate organic matter flux and planktonic new production in the deep ocean: Nature, v. 282, p. 677–680.
Finney, B. P., Lyle, M. W., and Heath, G. R., 1988, Sedimentation at MANOP site H (eastern equatorial Pacific) over the past 400,000 years: climatically induced redox variations and their effects on transition metal cycling: Paleoceanography, v. 3, p. 169–189.
Fischer, K., Ms, 1983, Particle fluxes in the eastern tropical Pacific Ocean—sources and processes. Ph.D. thesis, Oregon State University, Corvallis, p. 225.
Froelich, P. N., Klinkhammer, G. P., Bender, M. L., Luedtke, N. A., Heath, G. R., Cullen, D., Dauphin, P., Hammond, D., Hartman, B., and Maynard, V., 1979, Early oxidation of organic matter in pelagic sediments of the eastern equatorial Atlantic: Suboxic diagenesis: Geochimica et Cosmochimica Acta, v. 43, p. 1075–1090.
Goloway, F., and Bender, M. L., 1982, Diagenetic models of interstitial nitrate profiles in deep sea suboxic sediments: Limnology and Oceanography, v. 27, p. 624–638.
Gratton, Y., Edenborm, H. M., Silverberg, N., and Sundby, B., 1990, A mathematical model of Mn diagenesis in bioturbated sediments: American Journal of Science, v. 290, p. 242–262.
Guinasso, Jr. N. L., and Schink, D. R., 1975, Quantitative estimates of biological mixing rates in abyssal sediments: Journal of Geophysical Research, v. 80, p. 3032–3043.
Heath, G. R., and Lyle, M. W., 1982, Modification of hydrothermal sediment by suboxic diagenesis: evidence for Mn loss at MANOP site M (8°45′N, 104°W) (abstract): EOS, v. 63, p. 999.
Heggie, D., Kahn, D., and Fischer, K., 1986, Trace metals in metalliferous sediments, MANOP site M: interfacial pore water profiles: Earth and Planetary Science Letters, v. 80, p. 106–116.
Hem, J. D., 1981, Rates of Mn oxidation in aqueous systems: Geochimica et Cosmochimica Acta, v. 45, p. 1369–1374.

Jahnke, R. A., Emerson, S., Reimers, C., Schuffert, J., Ruttenberg, K., and Archer D., 1989, Benthic recycling biogenic debris in the eastern tropical Atlantic ocean: Geochimica et Cosmochimica Acta, v. 53, p. 2947–2960.

Jahnke, R. A., Heggie, D., Emerson, S., and Grundmanis, V., 1982a, Pore water of the central Pacific ocean: nutrient results: Earth and Planetary Science Letters, v. 61, p. 233–256.

Jahnke, R. A., Heggie, D., Emerson, S., and Murray, J., 1982b, A model of oxygen reduction, denitrification and organic matter mineralization in marine sediments: Limnology and Oceanography, v. 27, p. 610–623.

Jumars, P. A., and Wheatcroft, R. A., 1989, Responses of benthos to changing food quality and quantity, with a focus on deposit feeding and bioturbation, *in* Berger, W. H., Smetacek, V. S., and Wefer, G., editors, Productivity of the Ocean: Present and Past: New York, John Wiley & Sons, p. 235–253.

Kadko, D., and Heath, R. R., 1984, Models of depth-dependent bioturbation at MANOP site H in the eastern equatorial Pacific: Journal of Geophysical Research, v. 89, p. 6567–6570.

Kalhorn, S., and Emerson, S., 1984, The oxidation state of Mn in surficial sediments of the deep sea: Geochimica et Cosmochimica Acta, v. 48, p. 897–902.

Klinkhammer, G. P., 1980, Early diagenesis in sediments from the eastern equatorial Pacific, II. Pore water metal results: Earth and Planetary Science Letters, v. 49, p. 81–101.

Knowles, R., 1982, Denitrification: Microbiological Reviews, v. 46, p. 43–70.

Levin, L. A., Huggett, C. L., and Wishner, K. F., 1991, Control of deep-sea benthic community structure by oxygen and organic-matter gradients in the eastern Pacific ocean: Journal of Marine Research, v. 49, p. 763–800.

Li, Y. H., and Gregory, S., 1974, Diffusion of ions in sea water and in deep sea sediments: Geochimica et Cosmochimica Acta, v. 38, p. 703–714.

Li, Y. H., Guinasso, N. L., Cole, K. H., Richardson, M. D., Johnson, J. W., and Schink, D. R., 1985, Radionuclides as indicators of sedimentary processes in abyssal Caribbean sediments: Marine Geology, v. 68, p. 187–204.

Lyle, M., 1983, The brown-green color transition in marine sediments: a marker of the Fe(III)-Fe(II) redox boundary: Limnology and Oceanography, v. 28, p. 1026–1033.

Lyle, M., Heath, G. R., and Robbins, J. M., 1984, Transport and release of transition elements during early diagenesis: sequential leaching of sediments from MANOP sites M and H. Part I. pH 5 acetic acid leach: Geochimica et Cosmochimica Acta, v. 48, p. 1705–1715.

Marinelli, R. L., 1994, Effects of burrow ventilation on activities of a terebellid polychaete and silicate removal from sediment pore waters: Limnology and Oceanography, v. 39, p. 303–317.

McDuff, R. E., and Ellis, R. A., 1979, Determining diffusion coefficients in marine sediments: a laboratory study of the validity of resistivity techniques: American Journal of Science, v. 279, p. 666–675.

Messer, J. J., and Brezonik, P. L., 1983–1984, Laboratory evaluation of kinetic parameters for lake sediment denitrification models: Ecological Modeling, v. 21, p. 277–286.

Millero, F. J., Sotolongo, S., and Izaguirre, M., 1987, The oxidation kinetics of Fe(II) in sea water: Geochimica et Cosmochimica Acta, v. 51, p. 793–801.

Monod, J., 1949, The growth of bacterial cultures: Annual Review of Microbiology, v. 3, p. 371–394.

Morgan, J. J., 1967, Chemical equilibria and kinetic properties of Mn in natural waters, *in* Faust, S. D. and Hunter, J. V., editors, Principles and Applications of Water Chemistry: Chichester, Wileys, p. 561–626.

Muela, A., Gorostiza, I., Iriberri, J., and Egea, L., 1988, Indicative parameters of denitrification in river sediments: Acta Hydrochimica Hydrobiologica, v. 16, p. 157–163.

Murray, D. W., Ms, 1987, Spatial and Temporal variation in sediment accumulation in the central tropical Pacific: Ph.D. thesis, Oregon State University, p. 339.

Murray, J. W., and Kuivila, K. M., 1990, Organic matter diagenesis in the northeast Pacific: transition from aerobic clay to suboxic hemipelagic sediments: Deep Sea Research, v. 37, p. 59–80.

Myers, C. R., and Nealson, K. H., 1988, Microbial reduction of Mn oxides: Interactions with Fe and sulfur: Geochimica et Cosmochimica Acta, v. 52, p. 2727–2732.

Nakajima, M., Hayamizy, T., and Nishimura, H., 1984a, Effect of oxygen concentration on the rates of denitrification and denitrification in the sediments of a1. eutrophic lake: Water Research, v. 18, p. 335–338.

———— 1984b, Inhibitory effect of oxygen on denitrification and denitrification in sludge from an oxidation ditch: Water Research, v. 18(3), p. 339–343.

Pedersen, T. F., Vogel, J. S., and Southon, J. R., 1986, Copper and Mn in hemipelagic sediments at 21°N East Pacific Rise: Diagenetic contrasts: Geochimica et Cosmochimica Acta, v. 50, p. 2019–2031.

Postma, D., 1985, Concentration of Mn and separation from Fe in sediments-I. Kinetics and stoichiometry of the reaction between birnessite and dissolved Fe(II) at 10°C: Geochimica et Cosmochimica Acta, v. 49, p. 1023–1033.

Press, W. H., Teukolsky, S. A., Vetterling, W. T., and Flannery, B. P., 1993, Numerical Recipes in Fortran: The Art of Scientific Computing, 2d edition, Cambridge University Press, p. 963.

Price, B. A., Ms, 1988, Equatorial pacific sediments: A chemical approach to ocean history. Ph.D. thesis, Scripps Institute of Oceanography, University of California San Diego, p. 364.

Rabouille, C., and Gaillard, J. F., 1991a, A coupled model representing the deep sea organic carbon mineralization and oxygen consumption in surficial sediments: Journal of Geophysical Research, v. 96(C2), p. 2761–2776.

———— 1991b, Towards the Edge: Early Diagenetic Global Explanation. A model depicting the early diagenesis of organic matter, O_2, NO_3, *Mn* and PO_4: Geochimica et Cosmochimica Acta, v. 55, p. 2511–2525.

Reimers, C. E., Kalhorn, S., Emerson, S. R., and Nealson, K. H., 1984, Oxygen consumption rates in pelagic sediments from the Central Pacific: first estimates from microelectrode studies: Geochimica et Cosmochimica Acta, v. 48, p. 903–910.

Rhoads, D. C., 1974, Organism-sediment relations on the muddy sea floor: Oceanography and Marine Biology Annual Review, v. 12, p. 263–300.

Rhoads, D. C., and Morse, J. W., 1971, Evolutionary and ecological significance of oxygen-deficient marine basins: Lethaia, v. 4, p. 413–428.

Richter, R., 1952, Fluidal-texture, *in* Sediment-Gesteinen und uber Sedifluktion uberhaupt: Notizbl. Hess. L.-Amt. Bodenforsch., v. 3, p. 67–81.

Roache, P. J., 1982, Computational Fluid Dynamics: Albuquerque, New Mexico, Hermosa Publications, p. 446.

Robbins, J. A., 1986, A model for particle selective transport of tracers in sediments with conveyor belt deposit feeders: Journal of Geophysical Research, v. 91(C7), p. 8542–8558.

Rutgers van der Loeff, M. M., 1990, Oxygen in pore waters of deep-sea sediments: Philosophical Transactions of the Royal Society of London, v. A331, p. 69–84.

Sawlan, J. J., and Murray, J. W., 1983, Trace metal remobilization in the interstitial waters of red clay and hemi-pelagic sediments: Earth and Planetary Science Letters, v. 64, p. 213–230.

Schink, D. R., and Guinasso, Jr., N. L., 1977, Effects of bioturbation on sediment-seawater interaction: Marine Geology, v. 23, p., 133–154.

Smith, C. R., 1992, Factors controlling bioturbation in deep-sea sediments and their relation to models of carbon diagenesis, *in* Rowe, G. T. and Pariente, V., editors, Deep-Sea Food Chains and the Global Carbon Cycle: Kluwer, Amsterdam, p. 375–393.

Smith, C. R., Pope, R. H., DeMaster, D. J., and Magaard, L., 1993, Age dependent mixing of deep-sea sediments: Geochimica et Cosmochimica Acta, v. 57, p. 1473–1488.

Sorensen, J., 1987, Nitrate reduction in marine sediment: pathways and interactions with iron and sulfur cycling: Geomicrobiology Journal, v. 5, p. 401–420.

Stordal, M. C., Johnson, J. W., Guinasso, N. L., and Schink, D. R., 1985, Quantitative evaluation of bioturbation rates in deep ocean sediments. II. Comparisons of rates by ^{210}Pb and $^{239,240}Pu$: Marine Chemistry, v. 17, p. 99–114.

Stumm, W., and Morgan, J. J., 1981, Aquatic Chemistry: New York, Wiley-Interscience, p. 780.

Taylor, R. J., Ms, 1987, Mn geochemistry in Galveston Bay sediments: Ph.D. thesis, Texas A & M University, p. 258.

Ullman, J. W., and Aller, R. C., 1982, Diffusion coefficients in near shore marine sediments: Limnology and Oceanography, v. 27, p. 552–556.

Westrich, J. T., and Berner, R. A., 1984, The role of sedimentary organic matter in bacterial sulfate reduction: The G model tested: Limnology and Oceanography, v. 29, p. 236–249.

Wheatcroft, R. A., Jumars, P. A., Smith, C. R., and Nowell, A. R. M., 1990, A mechanistic view of the particulate biodiffusion coefficient: step lengths, rest periods and transport direction: Journal of Marine Research, v. 48, p. 177–207.

Wilson, T. R. S., Thomson, J., Colley, S., Hydes, D. J., Higgs, N. C., and Sorenson, J., 1985, Early organic diagenesis: The significance of progressive subsurface oxidation fronts in pelagic sediments: Geochimica et Cosmochimica Acta, v. 49, p. 811–822.

Yeats, P. A., and Strain, P. M., 1990, The oxidation of manganese in seawater: rate constants based on field data: Estuarine, Coastal and Shelf Science, v. 31, p. 11–24.